KU LEUVEN

FACULTY OF SCIENCE

Adaptational Regime Shifts in Space

A modelling approach.

Maxime Fajgenblat

Supervisor: Prof. dr. Luc De Meester
Ecology, Evolution and
Biodiversity Conservation

Mentor: Laurens J. Kilsdonk
Ecology, Evolution and
Biodiversity Conservation

Thesis presented in
fulfillment of the requirements
for the degree of Master of Science
in Biology

Academic year 2016-2017

Dankwoord

Mijn oprechte dank gaat in de eerste plaats uit naar mijn begeleider Laurens Kilsdonk en professor Luc De Meester. Na eerder mijn bachelorproef afgelegd te hebben onder hun hoede, was de keuze voor deze thesis voor de hand liggend. Bedankt Laurens, voor de vrijheid die je mij telkens gaf en voor je eindeloze enthousiasme om ideeën uit te wisselen tijdens de vele overlegmomenten. Bedankt Luc, voor de enorme inspiratie, en dit al sinds mijn eerste dag als student aan deze universiteit.

Ik wil ook graag de overige leden van het labo bedanken voor de warme ontvangst, de leerrijke gesprekken en de steeds grote bereidheid om te helpen.

Mijn ouders en mijn vriendin Jozefien, wil ik graag bedanken om deze drukke periode beduidend aangenamer te maken, ondanks het feit dat ik zelf weinig aanwezig was.

Contents

Summary IV

Samenvatting V

1 Introduction 1

1.1 Genetic variation in landscapes 1

1.1.1 Geographic distance as driver of genetic differentiation 1

1.1.2 Going beyond distance: the rise of landscape genetics 2

1.1.3 Microgeographic adaptation 2

1.1.4 Processes and patterns of differentiation in landscapes 4

1.2 Interactions between local adaptation and gene flow 5

1.2.1 Constraining effects of adaptive divergence on gene flow 5

1.2.2 Constraining effects of gene flow on adaptive divergence 6

1.2.3 Integrating interactions between gene flow and adaptive divergence 8

1.3 Regime shifts in ecology and evolution 8

1.3.1 Regime shifts in ecology 10

1.3.2 Regime shifts in evolution 11

1.3.3 Regime shifts in eco-evolutionary interactions 12

1.3.4 Regime shifts in landscapes 13

1.3.5 Evolutionary regime shifts at the landscape level? 16

1.4 Modelling adaptational regime shifts at the landscape scale 17

1.4.1 Monopolization and the window of opportunity 17

1.4.2 Neutral landscape models 18

2 Goals 20

3 Material and methods 21

3.1 Landscape generation 21

3.2 Population dynamics 23

3.2.1 Genome representation and reproduction 23

3.2.2 Fitness-dependent mortality 26

3.2.3 Migration 26
3.2.4 Stochastic extension for finite populations 27
3.3 Model output 28
3.4 General model exploration strategy 28
3.5 Numerical solving 29
4 Results and discussion 30
4.1 Three-deme metapopulations 30
4.2 Randomly distributed discrete niche type landscapes 34
4.3 Randomly distributed (semi-)continuous niche type landscapes 35
4.4 Multidimensional niche type landscapes 37
4.5 Aggregated niche type landscapes and synchronicity with refugia 39
4.6 Niche alterations in heterogeneous landscapes 40
4.7 Global findings 40
4.8 Further directions 41
5 References 42
Addendum 1: Risk analysis 1

Summary

Maladaptive gene flow can restrict the ability of populations to locally adapt in heterogeneous landscapes. However, local adaptation can enable populations to prevent gene flow, either through competitive advantages of well adapted phenotypes or through priority effects. The constraining effect of gene flow on adaptive divergence and the constraining effect of adaptive divergence on gene flow can result in a positive feedback mechanism and adaptational regime shifts. Depending on the dispersal rate, these regime shifts can result in populations that are either well- or maladapted and can undergo abrupt adaptational shifts. Mathematical models suggest the existence of such dynamics in simple systems. The aim of this thesis is to analyse whether these adaptational regime shifts can occur in spatially structured populations, by means of a modelling approach. We find that adaptational regime shifts persist and even are reinforced in heterogeneous landscapes. For low levels of dispersal, we find that subpopulations are able to resist gene flow to a high degree, until a critical threshold in dispersal is reached and one phenotype starts to dominate the entire landscape. We also find that heterogeneous niche types, niche multidimensionality and spatial aggregation of similar niche types can reinforce these patterns. Finally, our results also suggest that the systematic but gradual conversion of niche types into other niche types, can yield dramatic shifts in adaptational dynamics of populations.

Samenvatting

In heterogene landschappen kan gene flow het vermogen van populaties tot lokale adaptatie verminderen door de influx van onaangepaste allelen. Omgekeerd kan adaptatie populaties in staat stellen om gene flow te beperken, hetzij door het competitieve voordeel van lokaal geadapteerde residente individuen ten opzichte van immigrerende fenotypes, hetzij door prioriteitseffecten. Op die manier kan een positief feedbackmechanisme optreden tussen lokale adaptatie en gene flow, dat aanleiding zou kunnen geven tot adaptationele regime shifts. Deze houden in dat populaties, afhankelijk van de heersende connectiviteit tussen populaties, in een goede dan wel slecht geadapteerde toestand kunnen verkeren en abrupte shifts kunnen plaatsvinden wanneer veranderingen in connectiviteit optreden. Wiskundige modellen wijzen inderdaad op het optreden van dergelijke regime shifts in eenvoudige systemen. Deze thesis heeft tot doel om modelmatig na te gaan in welke mate deze fenomenen ook een rol zouden kunnen spelen in ruimtelijk gestructureerde populaties, en welke interacties hierbij optreden. We stellen vast dat deze regime shifts inderdaad kunnen optreden in landschappen en zelfs versterkt worden. Subopulaties zijn in staat om in grote mate weerstand te bieden tegen immigranten, tot een kritieke waarde in connectiviteit bereikt wordt en een enkel fenotype het hele landschap domineert. We stellen vast dat sterke verschillen in niche types, nichemultidimensionaliteit en de spatiale aggregatie van gelijkaardige niches deze effecten vergroten. Geleidelijke maar systematische omzettingen van een bepaalde niche in een andere niche in een landschap, kunnen eveneens tot abrupte transities leiden.

1 Introduction

Understanding the complex processes that drive genetic composition in natural populations has been a major focus of evolutionary biology and population genetics. While correlational approaches generally succeed in explaining some variance, a substantial proportion often remains unexplained. Regime shifts and trajectory-dependant mechanisms might in part underlie this lack of inferential power and gained increased attention in the study of biological patterns during the last decade.

We explore how regime shifts emerging from the interplay between local adaptation and gene flow genetically structure populations at the landscape level. By means of introduction, the following section provides an overview of our current understanding of (1) genetic variation in landscapes; (2) interactions between local adaptation and gene flow; (3) the prevalence of regime shifts in ecology and evolution and (4) the available modelling approaches to study adaptational regime shifts at the landscape level.

1.1 Genetic variation in landscapes

Ever since Darwin published his seminal work in 1859, natural selection has been viewed as one of the central drivers of genetic differentiation in natural populations. However, several other mechanisms are now known to oppose selective processes, and there is still ongoing debate on their relative importance. Neutral theory has advanced selectively neutral processes such as genetic drift and random gene flow as most important drivers of molecular evolutionary change (Kimura 1983; Endler 1986; Schluter 2000; Edelaar & Bolnick 2012). Together, both neutral and selective processes can cause different patterns of genetic differentiation at the landscape scale. We discuss several mechanisms that integrate both views in order to conceptualize the understanding of genetic differentiation in natural populations.

1.1.1 Geographic distance as driver of genetic differentiation

Sewall Wright was the first to acknowledge a major driver of genetic differentiation in landscapes by introducing the concept of Isolation by Distance (IBD; Wright 1943). IBD predicts an increase in genetic differentiation along with increasing geographic distance. In general, species ranges exceed the range covered by individuals by several orders of magnitude. For example, 99.5% of the seeds of the Dandelion (*Taraxacum officinale*), a well-known plant species capable of long-distance dispersal, land within 10 m of the mother plant (Tackenberg *et al.* 2003). Wright defined the *genetic neighbourhood* with an effective population size $N_e = 4\pi\sigma^2 d$, with σ the mean squared parent-offspring distance along one axis in continuous space and d the population density (Wright 1946). This neighbourhood is a circular area with radius 2σ within which movement and gene flow among individuals

is frequent enough to prevent genetic drift. Genetic neighbourhoods lead to a hierarchical pattern of changes in inbreeding coefficients among subgroups and hence, an increasing differentiation with increasing linear distance among subgroups. Patterns of Isolation by Distance are widespread in nature, since limitations in dispersal abilities are inherent to most species (Greenwood 1980; Jenkins *et al.* 2010).

1.1.2 Going beyond distance: the rise of landscape genetics

Isolation by Distance as a mechanism solely relies on restricted movement along a linear axis, ignoring other connectivity or environmental variables that might determine movement restrictions of individuals. A new discipline, landscape genetics, has emerged and addresses these shortcomings by bridging the fields of landscape ecology and population genetics (Manel *et al.* 2003). Landscape genetics "explicitly quantifies the effects of landscape composition, configuration and matrix quality on gene flow and spatial genetic variation" (Storfer *et al.* 2007). Landscape genetic studies aim at detecting genetic discontinuities and explaining these patterns by environmental features (Manel *et al.* 2003). The increasing availability of molecular genetic data and recent developments in spatial statistical methods have considerably advanced our knowledge on functional connectivity and the relative importance of environmental characteristics on adaptation (Manel & Holderegger 2013). In the majority of landscape genetics studies, environmental characteristics explain more genetic variation than Isolation by Distance patterns (Storfer *et al.* 2010). In addition to Isolation by Distance, the null model of differentiation, commonly identified spatial patterns are clinal patterns of variation, genetic boundaries to gene flow and, metapopulation structure, where differentiation is dominated by local extinctions and recolonizations (Manel *et al.* 2003).

1.1.3 Microgeographic adaptation

At microgeographic scale, gene flow is often assumed to genetically homogenize populations, overruling selection. Increasing evidence indicates the existence of

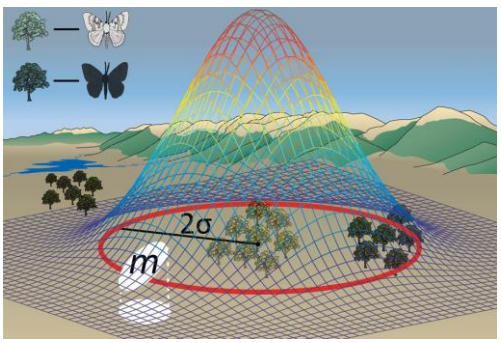

Figure 1. Dispersal kernel of a hypothetical moth species with corresponding genetic neighbourhood of radius 2σ (red circle). Microgeographic adaptation would apply when both colour morphs, each adapted to a particular tree type, co-occur within the same genetic neighbourhood. Reprinted from Richardson *et al.* (2014).

microgeographic variation in adaptation at small spatial scales, even within genetic neighbourhoods *sensu* Wright (1946). Richardson *et al.* (2014) identify seven mechanisms that increase selection strength or reduce maladaptive gene flow relative to dispersal, and can lead to microgeographic adaptation (Figure 1; Table 1).

Table 1. Overview of mechanisms that can cause microgeographic adaptation. Adapted from Richardson *et al.* (2014).

	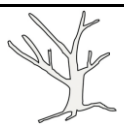	**Mechanism description**
Mechanisms capable of initiating divergence		
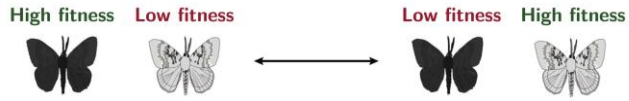		**Strong natural selection** conveys important fitness benefits for populations close to optimal phenotypes, reducing the impact of gene flow.
		**Landscape barriers** such as rivers, highways and unsuitable vegetation cover can restrict gene flow and cause differentiation at small scales.
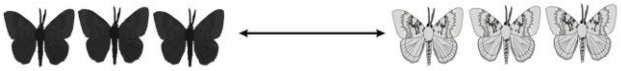		**Spatially autocorrelated natural selection** regimes lead to reduced levels of maladaptive gene flow compared to randomly distributed selective environments.
		**Habitat selection** and non-random distributions of genotypes over space, allow fine-scaled genetic differentiation that are enhanced rather than impeded by gene flow.
Amplifying mechanisms that require some prior divergence		
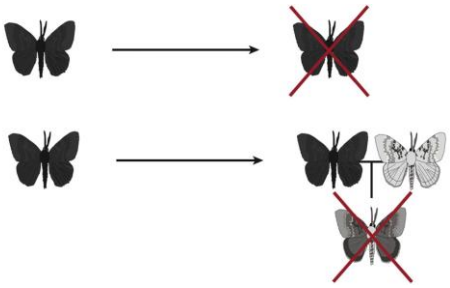		**Selective barriers** reduce the fitness of migrants before their alleles can be incorporated into the recipient gene pool. If mating can be realised, **post-zygotic selective barriers** may impose fitness or survival reductions to offspring (see below).
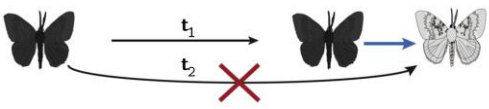		Adaptation of early colonists can create a barrier against future gene flow of maladapted alleles through **evolutionary monopolization effects** (see below).
		**Sexual selection** can prevent migrants to contribute to the local gene pool due to mating avoidance by resident individuals.

1.1.4 Processes and patterns of differentiation in landscapes

Orsini *et al.* (2013b) delineate a framework to link patterns of genetic differentiation in landscapes to a set of distinct processes. Several mechanisms causing microgeographic adaptation can be framed within this framework.

Isolation by Dispersal Limitation

Isolation by Distance (IBD) is a commonly found pattern in landscape genetic studies, but the identification of the underlying mechanism can sometimes be problematic (Meirmans 2012). Isolation by Distance as defined by (Wright 1943, 1946) corresponds to the process of Isolation by Dispersal Limitation.

Serial founder effects can also lead to patterns of Isolation by Distance. For example, the observed relationship between genetic differentiation and geographical distance in humans can be explained by serial founder effects following the range expansion which originated in Africa (Ramachandran *et al.* 2005). Therefore, caution is required in order to distinguish the underlying mechanisms, namely Isolation by Dispersal Limitation and Isolation by Colonization, and the resulting pattern, being Isolation by Distance (Orsini *et al.* 2013b).

Isolation by Adaptation

Selection acting in heterogeneous landscapes can promote a reduction in gene flow among populations. Local adaptation creates a selective barrier against migrants inhabiting ecologically different habitats. This results in a pattern of Isolation by Environment (IBE), caused by the mechanism of Isolation by Adaptation (IBA) (Orsini *et al.* 2013b). Under IBA, realised gene flow among dissimilar habitats will be restricted, in contrast to gene flow among similar habitats.

Isolation by Monopolization

Arrival order of genetic lineages and species can impact the resulting genotype and species composition of newly colonized patches or ecological opportunities (e.g. Mergeay et al. 2011, Orsini et al. 2013a, Ventura et al. 2014). Genetic and ecological priority effects are widespread and arise when early colonists gain a numerical advantage compared to subsequent immigrants with comparable fitness (Boileau *et al.* 1992; Kennedy *et al.* 2016). The founder effect (Mayr 1942) is a well-known genetic priority effect, which causes genetic differentiation due to random sampling of the regional genotype pool.

Provided sufficient time and standing genetic variation are available, early colonists might locally adapt and gain a competitive advantage over later arriving immigrants. This evolution-mediated priority effect is known as monopolization (De Meester *et al.* 2002, 2016). Monopolization can reinforce transient numerical priority effects by increased population growth and can even lead to long-term persistence of resident lineages.

Monopolization can arise both within metapopulation (population monopolization) and metacommunity contexts (community monopolization, Urban et al., 2008; Urban and De Meester, 2009) and through a wide range of spatiotemporal scales, ranging from metapopulations up to biogeography and speciation (De Meester et al., 2016) .

The occurrence of monopolization contests the widely held assumption that observed patterns in the distribution of genes and species do not depend on colonization history. Accordingly, an increased appreciation of monopolization and its consequences could benefit our understanding of a variety of topics, ranging from conservation and landscape genetics to biogeographical patterns (De Meester *et al.* 2016).

When founder events and thus colonization history affect genetic differentiation among populations, a pattern of Isolation by Colonization (IBC) arises. The interaction between founder events and selective processes can freeze transient priority effects, leading to Isolation by Monopolization (IBM). IBC and IBM yields a pattern of differentiation that is in principal independent of geographical or environmental distance. Successful monopolization however depends on the capacity of immigrants to invade a new patch within a window of opportunity. Depending on dispersal rates, invaders originating from ecologically similar patches are more likely to invade and monopolize the patch within the window of opportunity, yielding a possible weak signal of (historical) environmental conditions (Kilsdonk et al., *in prep.*).

1.2 Interactions between local adaptation and gene flow

During the last two decades, the reciprocal interactions between adaptive divergence and gene flow have received much attention (Hendry & Taylor 2004; Nosil & Crespi 2004; Räsänen & Hendry 2008). These studies specifically focused on Isolation by Adaptation as underlying mechanism. Evolutionary mediated priority effects, such as monopolization, provide an additional opportunity for gene flow and adaptation to interact. Under Isolation by Adaptation, gene flow among similar patches is still maintained. Isolation by Monopolization leads to an overall reduction in gene flow among all monopolized patches, due to rapid local adaptation (with respect to dispersal rates) to interpatch heterogeneities.

1.2.1 Constraining effects of adaptive divergence on gene flow

Both pre- and postzygotic mechanisms can contribute to reproductive barriers between distinct populations. Classical prezygotic mechanisms include dissimilar mating times (allochronic isolation), mating sites (habitat isolation), and courtship rituals or partner preferences (sexual isolation) (Dobzhansky 1937). More recently, prezygotic migrant inviability has been suggested as an important additional mechanism, comprising increased mortality of immigrants prior to mating or giving birth, compared to better adapted

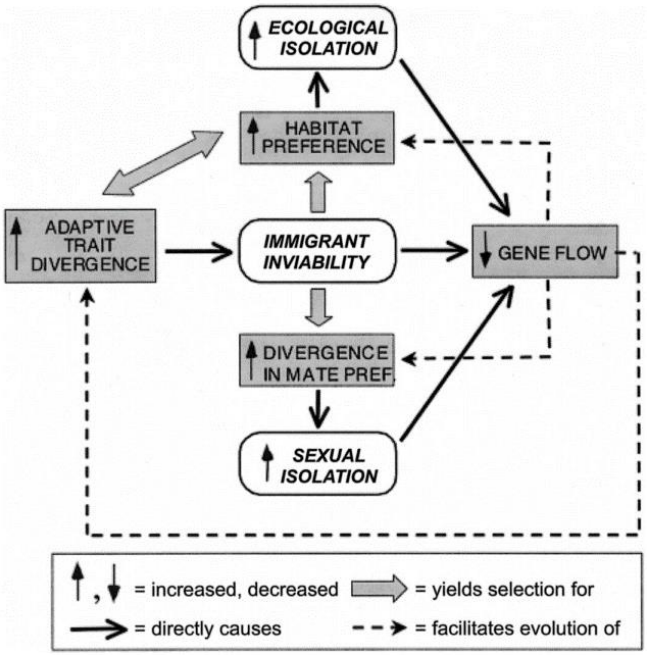

Figure 2. Direct and indirect effects of adaptive divergence on gene flow through immigrant inviability. Reprinted from Nosil et al. (2005).

residents (Figure 2; Nosil et al. 2005).

Postzygotic isolation is another major mechanism contributing to reduced levels of realised gene flow among different populations adapted to distinct environmental conditions (Rundle & Whitlock 2001). Two main forms of postzygotic isolation can be discerned. Intrinsic genetic isolation is the result of ecologically independent incompatibilities between individuals from different populations and the resulting offspring, e.g. due to the break-up of favourable epistatic interactions. In contrast, ecologically dependent isolation arises when hybrid individuals with intermediate phenotypes face a lack of intermediate environmental conditions, which comes at a severe fitness cost (Schluter 1996; Rundle & Whitlock 2001; Nosil 2004).

Studies providing direct evidence for the constraining effects of adaptive divergence on gene flow in natural systems are however rare (Räsänen & Hendry 2008).

1.2.2 Constraining effects of gene flow on adaptive divergence

The homogenising effect of gene flow can oppose natural selection by eroding the effects of selection (Slatkin 1987). The establishment of immigrant genotypes adapted to different ecological contexts can exert changes in allele frequencies in a direction opposite to natural selection. As such, undesirable alleles can persist in populations under the migration-selection balance, causing a *migration load* and decreasing mean population fitness. High levels of gene flow can induce extreme migration load, i.e. the loss of adaptive polymorphisms in populations, a phenomenon called *gene swamping* (Lenormand 2002).

Studies involving stream populations of the Threespine stickleback (*Gasterosteus aculeatus*) at both lake inlets (low levels of maladaptive gene flow from the lake population) and outlets (high levels of maladaptive gene flow from the lake population) provide strong evidence that gene flow can constrain adaptive divergence (Hendry & Taylor 2004; Moore & Hendry 2005; Moore *et al.* 2007). Experiments on walking-stick insects demonstrated negative effects of gene flow on demography, even countering the positive numerical effect of immigrants (Farkas *et al.* 2016).

On the island of Vlieland (NL), two subpopulations of Great tits (*Parus major*), separated by only a few kilometres, diverged significantly in clutch size due to higher levels of gene flow from the mainland in one of both subpopulations. The more isolated subpopulation performed considerably better in terms of offspring and general fitness, indicating negative effects of gene flow on adaptation (Postma & van Noordwijk 2005).

Populations can obviously also benefit from gene flow through evolutionary rescue (Gomulkiewicz & Holt 1995; Lopez *et al.* 2009; Gonzalez *et al.* 2012; Bourne *et al.* 2014). Moderate levels of gene flow can compensate for the loss of allelic diversity through drift processes and can increase the evolutionary potential of populations, which could be

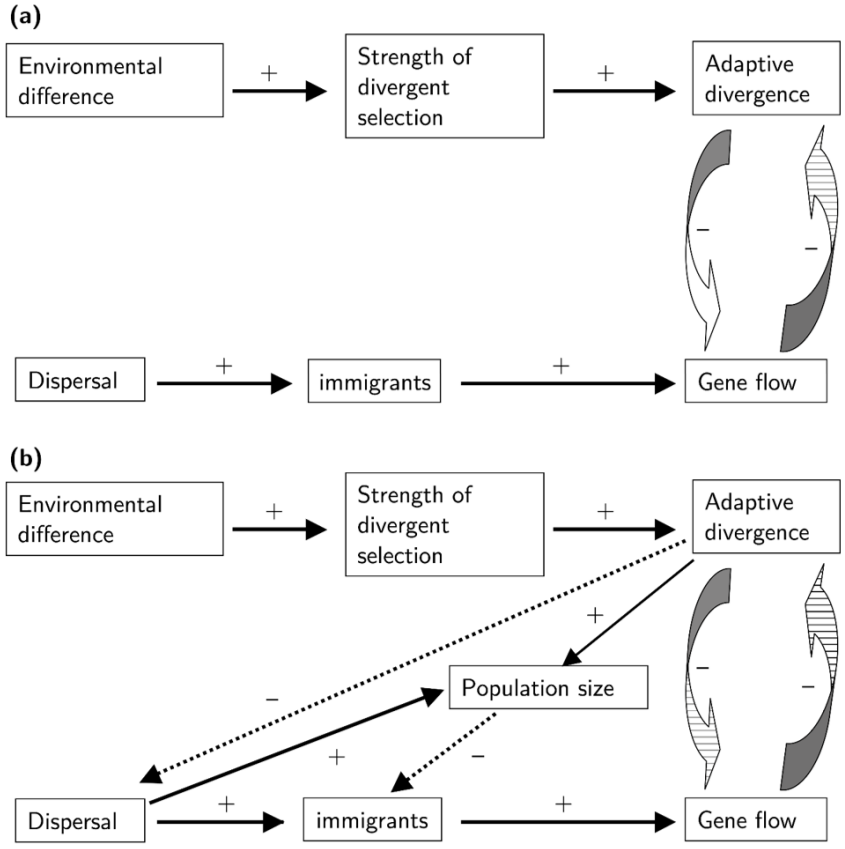

Figure 3. Interactions between adaptive divergence and gene flow. '+' symbols indicate a positive effect and '–' symbols indicate a negative effect in the direction of the arrow. Main effects are shown in (a), whereas additional relationships arising from dispersal and population size are shown in (b).
Adapted from Räsänen and Hendry (2008).

especially beneficial for small populations under changing environmental conditions (Lenormand 2002). In general, populations tend to benefit from gene flow when selection favours generalist phenotypes, while detrimental effects of migration load tend to dominate when selective conditions favour specialist phenotypes (Bourne *et al.* 2014). The complex balance between evolutionary rescue and migration load are especially challenging in conservation issues involving landscape fragmentation (Lopez *et al.* 2009).

1.2.3 Integrating interactions between gene flow and adaptive divergence

Both the constraining effect of gene flow on adaptive divergence and the constraining effect of adaptive divergence on gene flow (*ecological speciation*; Schluter 2000) are likely to contribute non-exclusively as causal agents to the frequently observed inverse relation between gene flow and adaptive divergence. Both mechanisms could generate a positive feedback loop (Figure 3) as suggested by for example Hendry and Taylor (2004), possibly resulting in regime shifts between near-complete adaptation versus near-complete maladaptation in populations (Räsänen and Hendry 2008).

1.3 Regime shifts in ecology and evolution

Ecosystems worldwide are facing unprecedented levels of environmental change through anthropogenic impact, including habitat fragmentation, climate change, invasive species and overexploitation (Butchart *et al.* 2010). Ecosystems are often considered to respond to changes in external conditions in a linear or gradual fashion, sometimes involving threshold values at witch abrupt changes proceed. Early theoretical work on ecosystem stability however suggested the existence of critical transitions and alternative stable states, which emerge when changing external conditions or perturbations undermine the resilience of ecosystems (Holling 1973; May 1977).

Currently, the theory of alternative stable states is well-established and very influential within the field of ecology (among others), and numerous instances have been identified and described in natural systems (Scheffer *et al.* 2001; Schröder *et al.* 2005). Critical transitions are often associated with dramatic ecological and economic consequences, which have prompted many efforts to identify early warning signals in recent years (Scheffer *et al.* 2009, 2012, 2015).

Alternative stable state theory predicts the presence of multiple stable states for a given condition. From a theoretical point of view, these distinct stable states are separated by an unstable equilibrium, which delineates the attraction basins of the stable equilibria (Figure 4). Necessary (although not sufficient) conditions for the existence of alternative stable states are positive feedback loops (Holling 1973), which are ubiquitous in natural systems (Crespi 2004).

Systems governed by alternative stable states show resilience against a changing environment due to feedback mechanisms. Resilience is here defined as the magnitude of perturbations a dynamical system can withstand without tipping over to an alternative state (*ecological resilience*; Holling 1973, 1996). Little changes in properties and functioning are observed by increasing levels of environmental change until a threshold or bifurcation point is reached and a catastrophic transition to the alternative state takes place. Since biological processes are never truly stable and fluctuations are always present, the use of the terms *dynamical regimes* and *regime shifts* instead of alternative stable states is more appropriate (Scheffer & Carpenter 2003).

Conditions at which regime shifts occur often differ for forward and backward shifts, a phenomenon known as hysteresis. This introduces trajectory dependency, since the ecosystem state is dictated by its history. Under hysteresis, the restoration of a system to its initial state can require reductions of the driver beyond the bifurcation point at which

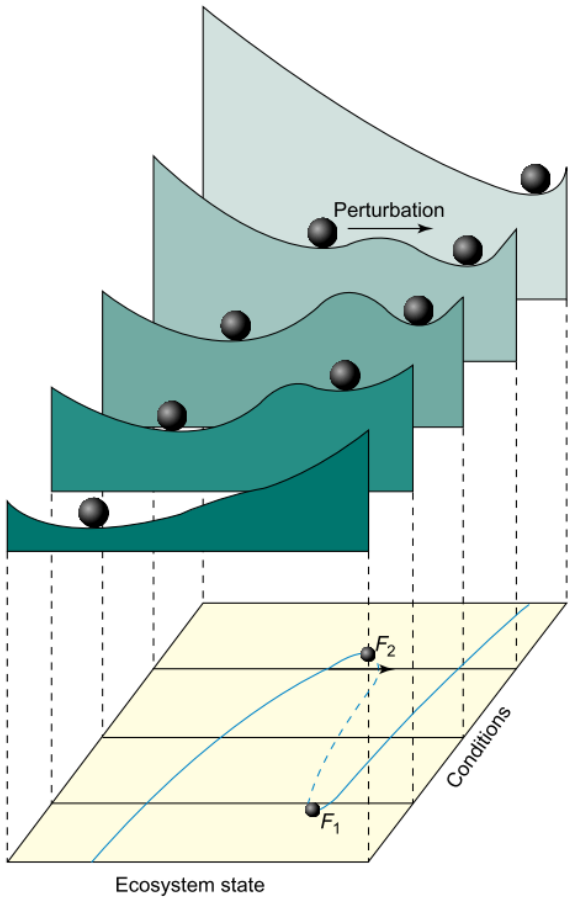

Figure 4. The valley landscape model conceptually represents the bistable relationship between ecosystem properties and environmental conditions. Hilltops represent unstable equilibria while valleys are stable equilibria, surrounded by slopes which can be seen as basins of attraction towards the valley. Under certain conditions, only a single possible ecosystem state might be possible (light and dark green). At intermediate conditions, two stable states exist, separated by an unstable equilibrium. Historical context determines the actual ecosystem state, which is stable and maintained unless perturbed or subject to further change beyond the bifurcation points (F_1 and F_2). Reprinted from Scheffer and Carpenter (2003).

the transition took place (Scheffer *et al.* 2001). In addition to the magnitude of environmental change and historical system properties, the regime of ecosystems might also be dictated by the rate of environmental change, i.e. a rate-induced critical transition could be triggered when the rate of change exceeds the capacity of systems to recover (Siteur *et al.* 2016).

1.3.1 Regime shifts in ecology

Clear versus turbid shallow lakes

The transition between clear, macrophyte rich water and turbid, algae dominated water in shallow lakes is one of the best-known examples of the occurrence regime shifts in nature (Scheffer 1990; Scheffer *et al.* 1993). Several underlying positive and negative feedback mechanisms result in sudden shifts in water clarity following increased levels of eutrophication (Smith *et al.* 1998). Oligotrophic lakes are typically characterized by clear water and rich submerged vegetations. Macrophytes are key in mediating nutrient load and inhibiting phytoplankton blooms through competition and the release of allelopathic substances (Van Donk & Van de Bund 2002). Clear water allows visual predators like piscivorous fish to control levels of herbivorous and planktivorous fish (Grimm 1989). This top-down control and the presence of refugia provided by macrophytes allows large zooplankton species to control the phytoplankton biomass (Jeppesen *et al.* 1997). Due to this set of self-stabilizing feedback mechanisms, increasing nutrient load (especially limiting phosphorus concentrations) initially does not affect the clarity of the lake. When the bifurcation point is reached as nutrient load further increases, the lake suddenly tips to the turbid state dominated by phytoplankton (Scheffer *et al.* 1993). In this state, macrophyte growth is inhibited by increased light attenuation by the phytoplankton. Herbivorous and planktivorous fish biomass increases due to the reduced hunting capacities of piscivorous fish. Due to increased predatory risk, the zooplankton community is now largely dominated by small individuals and species which less efficiently control phytoplankton biomass. Bottom feeding fish like Cyprinids contribute to an increased turbidity by resuspending sediment load (Meijer *et al.* 1990).

Transitions to turbid states following eutrophication negatively impact species composition and ecosystem services provided by the lake, and increases instances of toxic algae blooms. Due to hysteresis, nutrient load generally has to be reduced beyond the point at which the turbid state occurred in order to restore the initial state (Carpenter *et al.* 1999). Strong temporary reductions in fish biomass as *shock therapy* is an alternative measure which has been proven successful to restore the clear state in some cases (Søndergaard *et al.* 2007).

1.3.2 Regime shifts in evolution

Migrational meltdown

Alternative stable states and regime shifts have mainly been studied within the realm of pure ecology. So far, only a limited number of studies addressed the implications of evolutionary interactions in regime shifts (Ronce & Kirkpatrick 2001; De Roos *et al.* 2006; Williams & Lenton 2010; Lehtonen & Kokko 2012; Schreiber 2015), despite the multitude of positive feedback mechanisms observed in eco-evolutionary systems (Crespi 2004).

The theoretical models of Ronce and Kirkpatrick (2001) demonstrate the effects of gene flow on demographics and specialization of a species in heterogeneous, patchy landscapes, depending on the interplay with stabilizing selection. Small stochastic perturbations can lead to minor demographical asymmetries between populations, which are reflected in the degree of reciprocal exchange of migrant individuals. Populations receiving slightly more migrants undergo a mean fitness reduction due to the influx of maladapted genotypes (migration load), which further emphasizes demographic asymmetries. This positive feedback loop can induce source-sink dynamics among patches in heterogeneous landscapes. High levels of gene flow have a homogenizing effect on the genetic composition among patches and favour the evolution of generalists. Specialist species with narrow niche breadths only evolve at intermediate dispersal rates. In specialist systems, small increases in habitat connectivity can lead to a complete collapse of populations in one of the two habitat types. This process of *migrational meltdown* is similar to mutational meltdown, when maladaptation arises due to accumulation of mutations in small populations which feeds a positive feedback due to the negative effects of mutation load on demography (Lynch & Gabriel 1990). Moreover, the model system displays hysteresis and indicates small changes in landscape structure may have irreversible effects on the evolution speciation, such as the inability of specialist species to revert back to a generalist status.

Accordingly, historical factors may play an important role in structuring life history and distribution of populations and species. These findings also challenge the widely held belief that increases in gene flow are beneficial to population demography (Ronce & Kirkpatrick 2001).

This model system closely matches observed patterns in the North-American butterfly *Euphydryas editha*. This species underwent a drastic switch in host plant after all larvae feeding on the preferred host plant *Collinsia* died due to exceptional summer frost. In subsequent years, the species did not recolonize this niche, indicating a remarkable shift in source-sink dynamics and niche preference (Boughton 1999). The mechanism of migrational meltdown might also partially explain constraints on species ranges due to the detrimental effects of migration in typically small edge populations (Bridle & Vines 2007).

Tipping points in the dynamics of speciation

A long-standing debate in evolutionary biology concerns the pace of evolutionary change and speciation. Darwin considered speciation as a gradual and continuous process, where small changes build up over time and lead to gradual divergence between groups. In sharp contrast, 20th century evolutionary biologists like Gould posited the concept of *punctuated equilibria*. Inspired by the sudden emergence of new species in paleological records, they believed evolution acts in bursts and rather discontinuously.

Flaxman *et al.* (2014) and Nosil *et al.* (2017) propose a model of speciation involving tipping points between one and two species states. In a system under increasing divergent selection and high migration rates, they identify alternative stable states in differentiation. Initially, disruptive selection on the genomes and the build-up of linkage disequilibrium (LD) between populations increases only slowly, due to the homogenising effect of gene flow. Once a critical level of distruptive selection and LD is reached, differentiation is strongly accelerated due to a positive feedback loop between disruptive selection and LD, causing indirect selection on large parts of the genome through statistical associations among loci. A drastic drop in gene-flow due to increasingly differentiated genomes leads to a sudden transition to two species (Flaxman *et al.* 2014; Nosil *et al.* 2017).

1.3.3 Regime shifts in eco-evolutionary interactions

Within the monopolization framework, varying levels of dispersal between populations might also give rise to regime shifts (De Meester *et al.* 2016), similar to the hypothesized regime shifts at the interface between adaptive divergence and gene flow (Räsänen & Hendry 2008).

Given one focal population of individuals in a patch with low levels of interpatch dispersal, individuals inhabiting this patch will probably be able to fully adapt to the patch

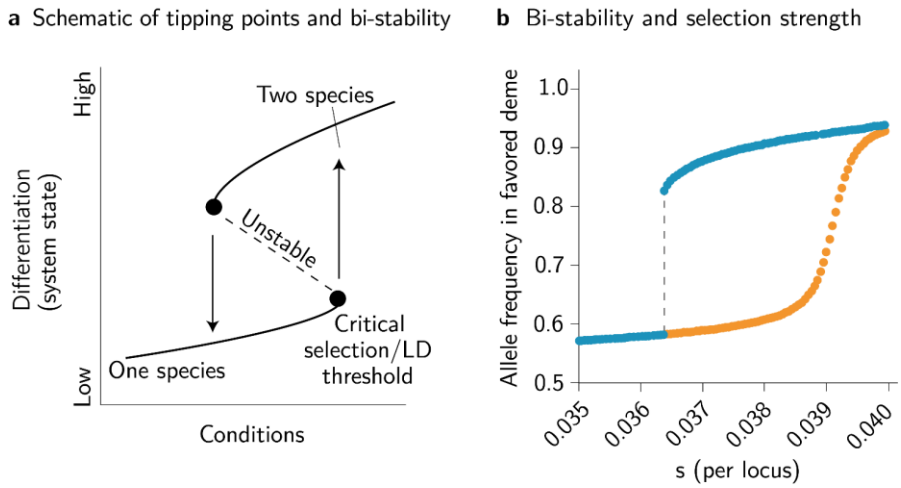

Figure 5. Bistability of speciation dynamics: depending on trajectory. Reprinted from Nosil *et al.* (2017).

conditions and successfully reduce gene flow of immigrant genotypes. When interpatch dispersal is increased, the patch remains monopolized due to the numerical and competitive advantage of the residents. When interpatch dispersal reaches a threshold value, some immigrant genotypes might establish due to mass effects. Gene flow from external populations will likely be maladaptive, given the well adapted resident population. In sexual populations, increasing dispersal will thus decrease the degree of adaptation of the population, thereby initiating a positive feedback loop. The superiority of residents is gradually weakened, allowing higher levels of realised gene flow, resulting in a population of maladapted individuals (Figure 6).

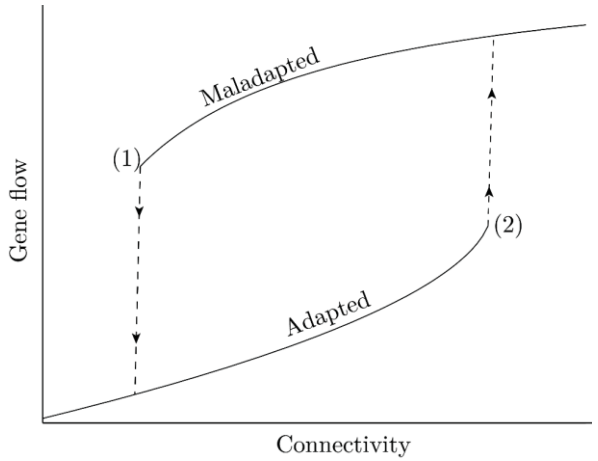

Figure 6. Regime shifts in gene flow levels depending on population connectivity. Full lines indicate stable adaptive regimes. Bifurcation points (1) and (2) indicate at which connectivity level transitions to the alternative state occurs. Reprinted from De Meester et al. (2016).

Subsequent reductions of interpatch dispersal initially will not restore the adapted state since maladapted immigrants continue to establish and prevent successful local adaptation. Once dispersal is low enough to enable local adaptation, the population switches back to the adapted state, through the mutually reinforcing processes of increased adaptation and reduced gene flow.

1.3.4 Regime shifts in landscapes

Most ecological phenomena involving regime shifts are studied in uniform and isolated systems. One may wonder whether regime shifts persist in more realistic, heterogeneous and spatially extended landscapes. Studies addressing these questions are scarce (Van de Koppel *et al.* 2002; Van Nes & Scheffer 2005; Hilt *et al.* 2011; Bel *et al.* 2012; Van De Leemput *et al.* 2015). Therefore, the theoretical expectation of regime shifts in eco-evolutionary interactions in one or two deme systems leads to the question if the same patterns apply at the landscape scale too. Local, intrapatch patterns might either cancel or reinforce each other at regional scale. In this section, we discuss available knowledge on the occurrence of regime shifts in spatially extended systems and heterogeneous landscapes

as well as relevant concepts that might interact with eco-evolutionary interactions at the landscape scale.

Positive feedback mechanisms are key to anticipate regime shifts in isolated systems. However, within a complex network of interactions, connectivity and heterogeneity between different nodes are generally seen as the main determinants of systemic stability. In heterogeneous networks with low connectivity, transitions are likely to occur independently at each node at different levels of environmental change, yielding rather gradual transitions at the system level. However, in more homogeneous and connected networks, the state of each node is likely to be dependent of the state of neighbouring node. Perturbations beyond a critical point will trigger a systemic critical transition (Figure 7; Scheffer et al. 2012). These patterns apply to for example mutualistic interactions, but other network interactions lead to different consequences. In competitive interactions, networks are more robust when nodes are compartmentalized into loosely connected modules (Scheffer *et al.* 2012). Hence, in addition to network topology, it is important to consider network interactions as well.

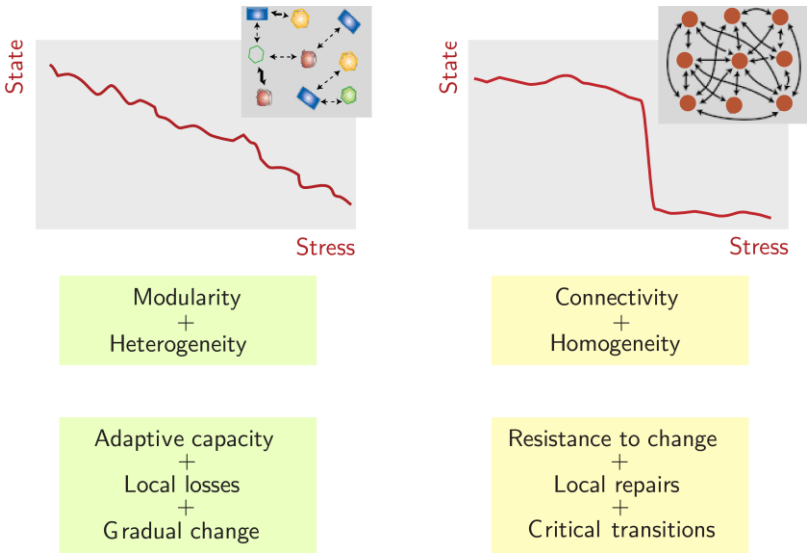

Figure 7. Overview of the influence of connectivity and homogeneity on state transitions. Systems with incomplete connectivity and heterogeneity tend to behave gradually compared to homogenous, highly connected networks. Dynamics can be altered based on the interaction type between nodes. For example, competitive interaction will result in opposite patterns. Adapted from Scheffer et al. (2012).

Van Nes & Scheffer (2005) integrate unidimensional spatial gradients of heterogeneity in model systems with known regime shifts. These systems show hysteresis under environmental heterogeneity in absence of dispersion (of matter and organisms) between patches, even though systemic responses are gradual in response to external stressors. In systems with interpatch dispersion and a randomly distributed heterogeneous environmental variable, catastrophic transitions and hysteresis persist surprisingly. In systems with a smoothly varying environmental variable, hysteresis largely disappears and

the response is rather gradual. In these systems, domino-effects occur: the alteration of one patch leads to a transition in neighbouring patches (Van Nes & Scheffer 2005).

Sharp boundaries between different regimes are frequently observed within continuous habitats, e.g. clear and vegetated zones in otherwise turbid shallow lakes (Figure 8; Scheffer et al. 1994) and the presence and absence of mussel beds in intertidal zones (Donahue *et al.* 2011). These observations initially lead to the belief that different regimes can co-exist in spatial configurations. Recent theoretical work however suggests the absence of hysteresis and the existence of only one dominant state in continuous landscapes depending on the environmental driver, to which the system always reverts (Van De Leemput *et al.* 2015). Beyond a critical value, the Maxwell point, perturbations will trigger a systemic shift to the alternative dominant regime. Close to the Maxwell point, the travelling wave of reversal to the dominant state is the slowest and both states can co-occur temporarily. This could provide an explanation for the observed co-occurrence of different regimes in continuous landscapes. Mild landscape barriers might as well lead to the co-occurrence of alternative regimes, even permanently (Van De Leemput *et al.* 2015).

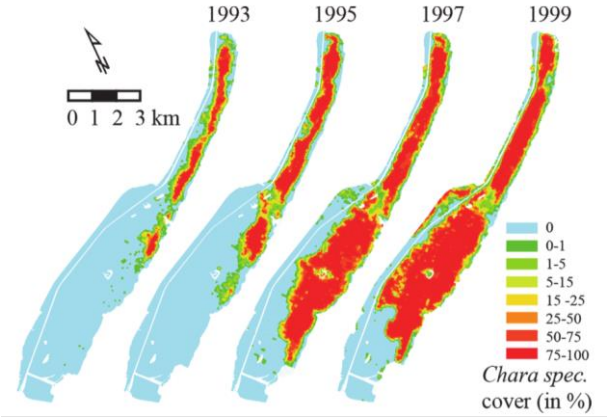

Figure 8. In the early '90s, sharp transitions between turbid zones and clear zones dominated by *Chara* sp. were observed in Lake Veluwe (NL) and seen as evidence for the simultaneous coexistence of multiple states (Scheffer *et al.* 1994). In following years, a lake-wide shift towards a clear, *Chara*-dominated state took place, providing evidence for the existence of a single dominating state given the governing conditions to which perturbations revert to. Reprinted from Van De Leemput *et al.* (2015).

In contrast to findings in continuous systems, studies on invasion dynamics demonstrated the co-existence of alternative equilibria in adjacent, discrete patches with sharp transitions due to Allee effects, fitness reductions at low population densities (Keitt *et al.* 2001; Holt *et al.* 2005). When mutually reinforcing effects occur in neighbouring patches of different states, self-organizing patterns can arise, which also lead to the co-existence of alternative regimes. These systems are characterized by scale-dependent feedbacks, and are for example observed in "tiger bushes" in arid regions (Figure 9), involving facilitation at small scales and competition at larger scales (Van de Koppel *et al.* 2002; Kéfi *et al.* 2016).

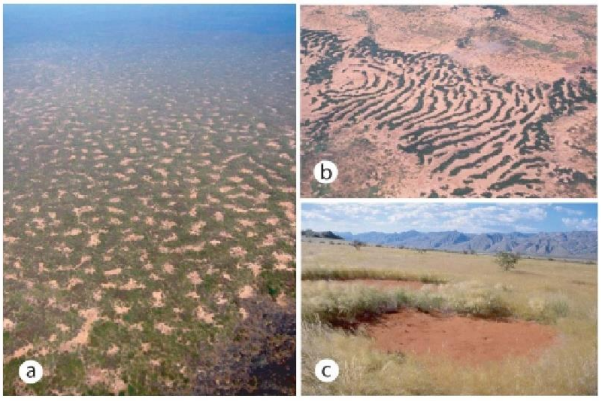

Figure 9. Examples of self-organizing vegetation patterns ("tiger bush") in arid regions: (a) "labyrinth" bushes; (b) striped "tiger" bushes and (c) dotted "leopard" bushes.
Image courtesy of J. Vergeer.

1.3.5 Evolutionary regime shifts at the landscape level?

In heterogeneous landscapes with discrete habitat types, populations are likely to reside on adaptive peaks under adaptive divergence. Hybridization will lead to intermediate phenotypes that fall between the different niches if intermediate niches are non-existent (Schluter 1996). The production and invasion of hybrids will either be rendered impossible or against a fitness cost, depending on the selection-migration balance in each patch. At the landscape level, this dependency might yield non-trivial interactions. For instance, in isolated patches, only phenotypes with slight deviations from optimal trait values can persist under the selection-migration balance. However, phenotypes with a slight deviation from optimal trait values do not exist in landscapes with homogeneously low levels of gene flow, since strong disruptive selection excludes F1-hybrids and thus the possibility of creating Fn-hybrids with more subtle deviations from optimality. However, in landscapes with spatial variations in gene flow among patches, these phenotypes can originate from adjacent patches with different selection-migration balances. This could yield the propagation (domino-effect) of a maladaptation wave along a gradient of decreasing connectivity, causing unexpected deviations from optimal trait values.

When optimal trait values vary linearly along one dimension through the landscape, mean population trait values are expected to perfectly coincide with optimal trait values, regardless of the level of gene flow, since equal influx of opposed phenotypes from both sides cancel each other out, as long as population densities are equal among patches and gene flow is homogeneous (Felsenstein 1977).

Niche multidimensionality increases landscape heterogeneity and is therefore expected to promote adaptive divergence between populations (Rice & Hostert 1993; Nosil & Sandoval 2008) and enhance monopolization.

1.4 Modelling adaptational regime shifts at the landscape scale

1.4.1 Monopolization and the window of opportunity

The time lag between the arrival of first colonists and subsequent immigrants can determine whether a system can be monopolized (De Meester *et al.* 2016; Vanoverbeke *et al.* 2016). By means of a model derived from the Lotka-Volterra equations for competition,

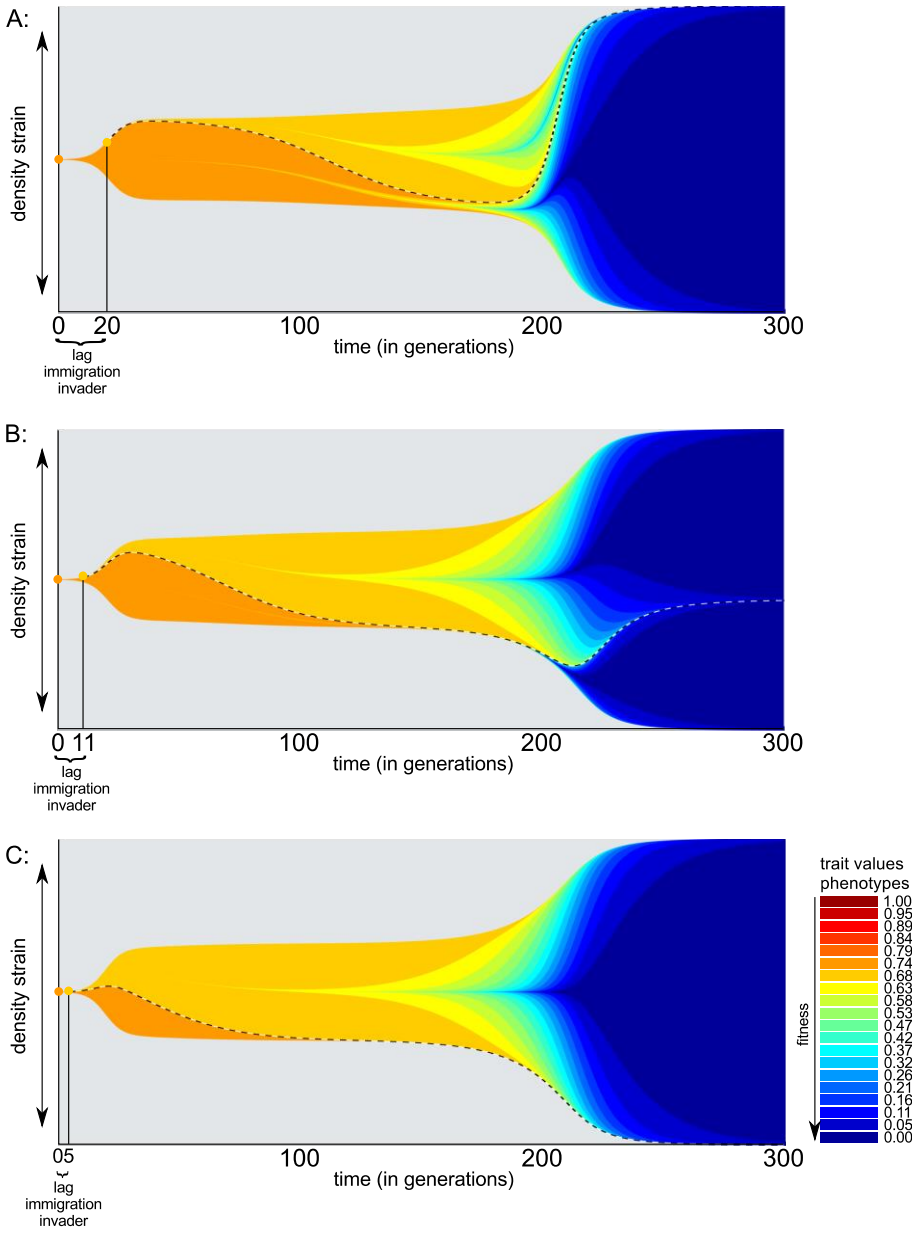

Figure 10. Muller plots representing the succession of phenotypes and lineages in a system after colonization and subsequent immigration. The colour spectrum is an indication for phenotype fitness, with dark blue as the optimally adapted phenotype. Dots represent immigration events. In (A), a time lag of 20 generations between colonization and subsequent immigration entirely prevents the establishment of the immigrant lineage, even though the invader has a superior fitness. In (B), a time lag of 11 generation allows partial establishment of the immigrant lineage. In (C), a time lag of only 5 generation does not allow monopolization by the initial colonizers. Reprinted from Kilsdonk *et al.* (*in prep.*).

Kilsdonk *et al.* (*in prep.*) show that small differences in arrival time can drastically alter the window of opportunity for immigrants following prior colonization, even if these immigrants are better adapted to local conditions (Figure 10). This thesis builds upon this theme by studying the mechanisms that maintain or cancel monopolization after the window of opportunity has closed.

1.4.2 Neutral landscape models

Neutral landscape models are grid-based null models of ecological complexity and have been intensively used in the study of ecological processes at the landscape scale (Gardner *et al.* 1987). We derived a comprehensive overview of simple and abstract landscape characteristics, along with examples of matching neutral landscape models, which are relevant in the study of eco-evolutionary interactions at the landscape scale (Table 2).

Table 2. Comprehensive overview of landscape patterns of interest and examples of corresponding occurrences in nature. Visual representations were randomly generated.

Patch distr.	Niche distr.	Niche axis	Visual representation	Examples of occurrences in nature	
random	random		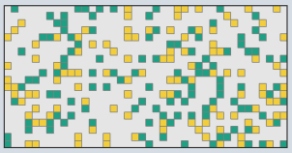	Clear and turbid ponds Non-fish and fish ponds	
random	random		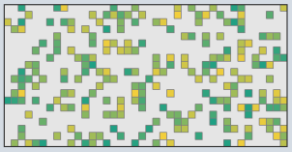	Patches at different successional stages	
random	random but biased		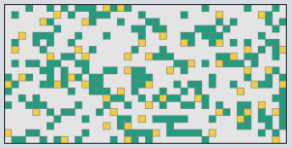	Resources suitable for generalists vs specialists Natural differences in the scarcity of habitat types	
random	linear gradient		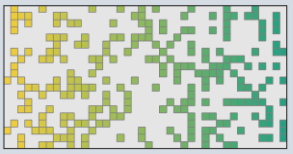	Latitudinal temperature gradients Salinity gradients in estuarine systems	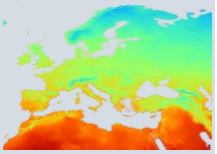
random	linear gradient + refugia		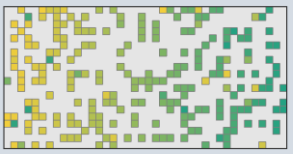	Urban heat islands Refugia Elevational temperature gradients Slope orientation	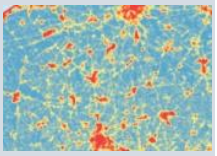
random	auto-correlated		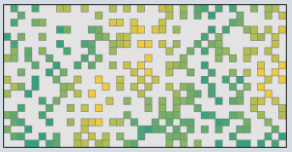	Most environmental variables are autocorrelated	
linear gradient	random		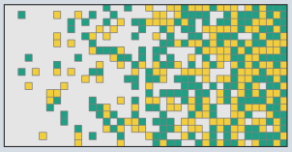	Gradients of anthropogenic influence (e.g. destruction) Populations often become smaller and more fragmented as species approach their ecological limits (Brown *et al.* 1995; Thomas & Kunin 1999) Island proximity to mainland	
linear gradient	random		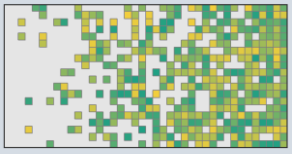		
random	random		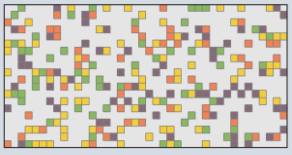	Often, more than one independent variable determines environmental conditions (Nosil & Sandoval 2008)	

2 Goals

The general aim of this thesis is to conceptualize and to generate qualitative predictions regarding how interactions between local adaptation and gene flow behave in different landscape scenarios, and to explore potential implications for conservation. We develop a new model by spatially integrating a previous extension of the competitive Lotka-Volterra equations between genotypes (Kilsdonk et al. *in prep.*). In this model, genotypes are capable of evolving within an explicit multilocus genetic system and migrating among patches. Using simulations, we explore the effects of landscape connectivity and heterogeneity on model predictions regarding realised gene flow among patches. Specifically, we aim at solving following questions:

- Do adaptational regime shifts persist in spatially structured populations?
- Can patches with near-complete adaptation and near-complete maladaptation of populations co-occur in landscapes? Or does one of both regimes dominate the landscape depending on dispersal rates? Do these systems show hysteresis?
- Does the type of niche axis (continuous or discrete) influence adaptation-gene flow patterns? Continuous niche axes (e.g. temperature, salinity or successional gradients) provide intermediate niches and might provide stepping stones for gene flow among patches for otherwise maladapted intermediate phenotypes, as compared to discrete niche axes (e.g. turbid and clear shallow lakes).
- Does the distribution of niche types (e.g. autocorrelated, aggregated) affect observed patterns?
- Does niche multidimensionality increase the likelihood of reduced chances of maladaptive gene flow in landscapes?
- How does a metapopulation react to gradually induced changes in selective environments?

3 Material and methods

The model we present comprises both a landscape and population dynamic part. The former defines the spatial configuration and characteristics of patches and the latter describes the dynamics of the sexually reproducing subpopulations inhabiting each patch. Subpopulations are considered to be discrete. Both model parts are linked through the processes of interpatch migration and niche-dependant performance of phenotypes. In the next sections, we outline the general procedures used for the generation of landscape models, we thoroughly describe the population dynamic part and present the approach used for the exploration of the model.

3.1 Landscape generation

We randomly generated spatially explicit abstract landscapes based on a based on a predefined set of rules. Landscapes consist of a regular lattice of evenly spaced patches. Default landscape size is 20×10 patches.

A niche type is accorded to each patch. Spatial variation in niche types reflects variations in biotic and abiotic conditions. Niche values range from 0 to 1, either in a discrete (e.g. Figure 11.a) or continuous fashion (e.g. Figure 11.c).

Niche space can be unidimensional (e.g. Figure 11.a) or two-dimensional (e.g. Figure 11.d), in order to accommodate for independent combinations of more than one niche axis (e.g. combined temperature and precipitation gradients). Individuals can adapt independently

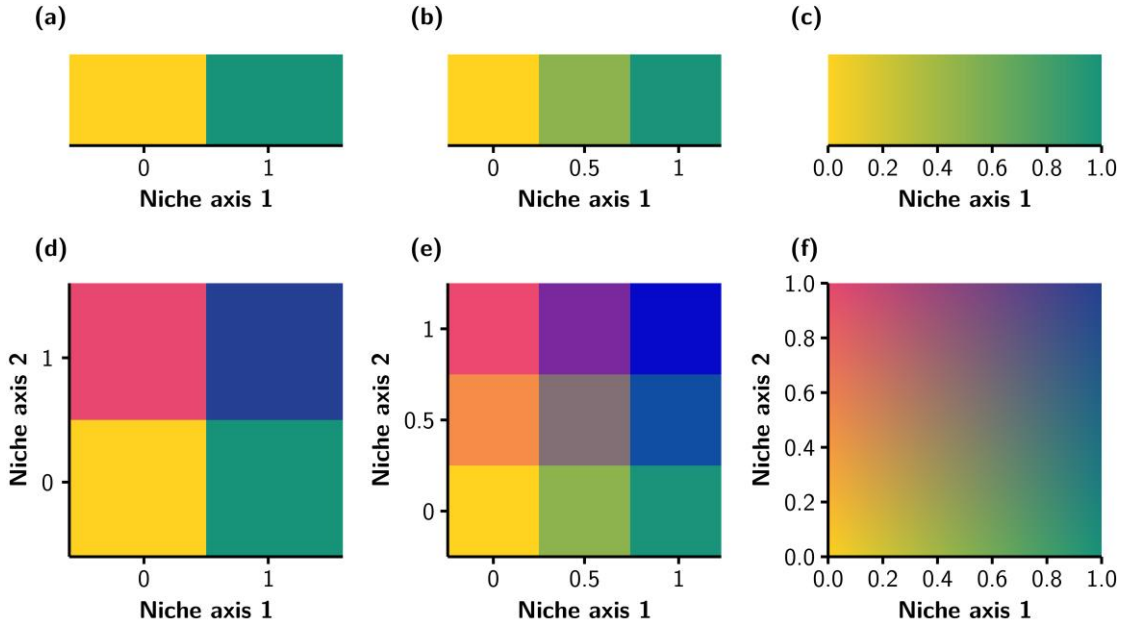

Figure 11. Different niche spaces can be used for the generation of random landscapes: (a) discrete binary and unidimensional niche space, (b) discrete ternary and unidimensional niche space, (c) continuous unidimensional niche space, (d) discrete binary and two-dimensional niche space, (e) discrete ternary and two-dimensional niche space and (f) continuous two-dimensional niche space.

along each niche axis. We restrict the number of niche axes in our simulations to 1 and 2.

The probability of a particular niche value being accorded to a patch can either be uniform or varying throughout the landscape. Spatially autocorrelated niche patterns are created by predefining the niche type of a randomly selected fraction of patches and by calculating niche values of remaining patches by local polynomial regression fitting interpolation using the `loess` function of the `stats` package (R Core Team 2016), under default settings. The strength of spatial autocorrelation depends on the fraction of initially selected patches before interpolation. Landscapes with spatially aggregated niche types are obtained by categorizing a spatially autocorrelated niche values into a discrete number of patch types. Refugia can be incorporated by altering the niche type of randomly selected patches.

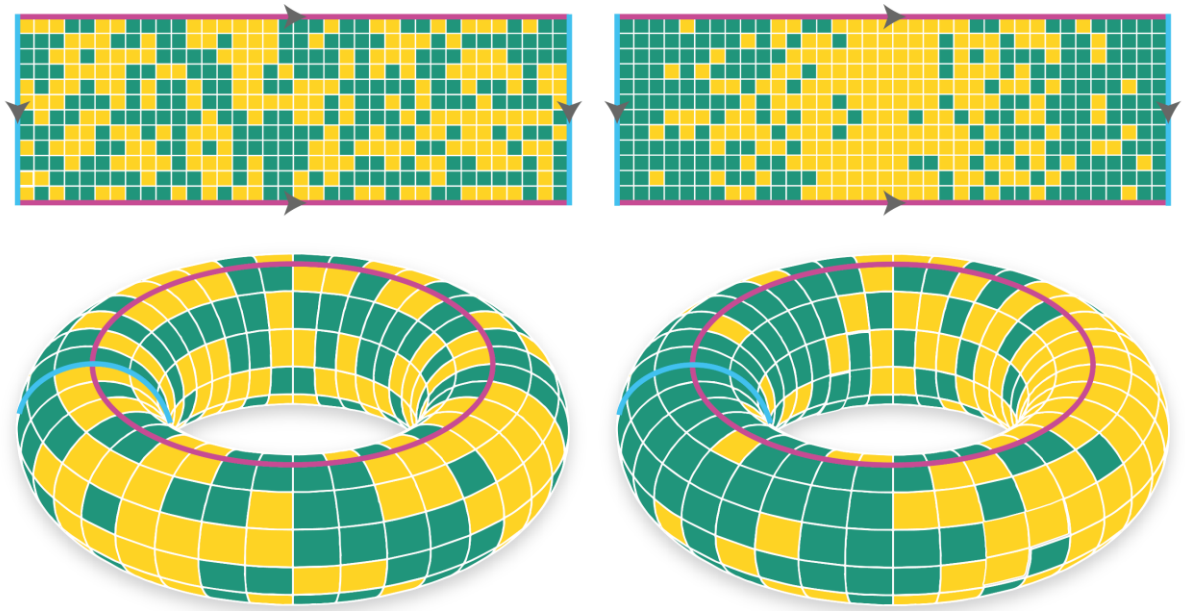

Figure 12. Flat (above) and corresponding torus representation (below) of two generated landscapes. Landscape edges with identical colours and arrowheads pointing in the same direction are joined in order to form a torus shaped landscape. The second landscape (right) is characterized by a gradient in niche type probability. This gradient is symmetrical in order to allow a continuous transition when wrapped into a torus.

For each generated landscape, a pairwise centroid-to-centroid distance matrix of all patches is calculated. Both Euclidean and torus distances can be calculated. Torus distances are calculated by wrapping landscapes vertically and horizontally into a doughnut-like object (Figure 12), in order to avoid edge effects. We exclusively use the torus shaped landscapes in our simulations. However, in the following, landscapes will be graphically presented using the flat representation for simplicity. Whenever present, gradients (e.g. in patch or niche distribution) are symmetrical with respect to their direction (i.e. horizontal in our landscape models), in order to allow continuous transitions when edges are wrapped together. Spatial autocorrelated niche patterns are also continuous at landscape edges.

3.2 Population dynamics

We developed a dynamical genetic-metapopulation model in `R` (R Core Team 2016), building on a prior extension of the Lotka-Volterra equations by Kilsdonk et al. (*in prep.*).

In our model, the metapopulation is structured based on three properties: (1) the genotype g, (2) the patch p they belong to and (3) the lineage l. A three dimensional array $\boldsymbol{N}$ with elements $N_{g,p,l}$, describes the densities of the different groups of the metapopulation:

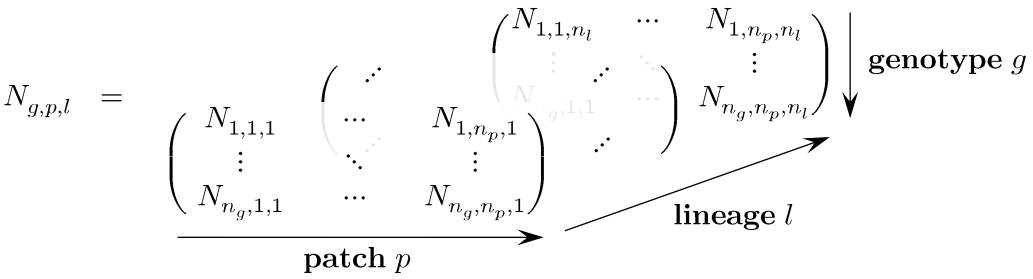

where $\mathrm{n_g}$ is the number of genotypes, n_p is the number of patches and n_l is the number of lineages. The dynamics of the metapopulation $\boldsymbol{N}$ are due to sexual reproduction (growth, recombination and mutation), migration and fitness-dependent mortality:

$$\forall g \in \{1,\dots,n_g\}, p \in \{1,\dots,n_p\}, l \in \{1,\dots,n_l\}:$$

$$\frac{dN_{g,p,l}}{dt} = r\mathrm{R}\ \boldsymbol{N}\ _{g,p,l}\left(1 - \sum_{i=1}^{n_g}\sum_{j=1}^{n_l} N_{i,j,p}\Big/K_p\right) - \mathrm{M}(N_{g,p,l}) - m_g N_{g,p,l}$$

where $r = 0.01$ is the intrinsic growth rate, $\mathrm{R}\ x\ $ is the reproduction function (see below), $K_p = 1$ is the carrying capacity in each patch, $\mathrm{M}(x)$ is the migration function (see below) and m_g is the mortality matrix representing the mortality of each genotype g in each patch p (see below). Population sizes $N_{g,l,p}$ are expressed as a fraction of the carrying capacity of each patch, as K_p equals one. In the following sections, we define the haploid and diploid reproduction models that can be used to calculate $\mathrm{R}\ x\ $, the dispersal model to calculate $\mathrm{M}(x)$, the calculation of the mortality matrix m_g and a stochastic extension to the model.

3.2.1 Genome representation and reproduction

Genomes are constructed as n sets of a unlinked loci that code for n quantitative traits, where n is the number of niche axes. Loci are biallelic ("0" and "1" alleles) and have an additive effect on the phenotypic trait, which ranges from 0 to 1 and is calculated as the fraction of "1" alleles across all loci of a particular set. We assume the absence of factors contributing to phenotypic trait values other than additive genetic effects.

The reproductive function $\mathrm{R}_{g,p,l}(\boldsymbol{N})$ takes the population array $\boldsymbol{N}$ as input and returns an offspring array. Multiplication by the intrinsic growth rate r and the density-dependent

term yields the rate of population change $dN_{g,p,l}/dt$ caused by reproduction.

We developed both a haploid and diploid multilocus model of sexual reproduction, assuming assortative mating through the production of a gamete pool, Mendelian segregation and free recombination.

Hypergeometric haploid multilocus model

In the haploid model, a alleles yield $n_g = a + 1$ different genotypes and hence, phenotypes. The gamete frequency pool matrix $Q_{g,l}$ is calculated by multiplying a mutation matrix $\boldsymbol{Y}$ by the patch population matrix $N_{g,l}$:

$$Q_{g,l} = \frac{Y_{g,g_{old}} \times N_{g,l}}{\sum_g \sum_l \left(Y_{g,g_{old}} \times N_{g,l} \right)}$$

where $\mathrm{Y_{g,g_{old}}} = \mathrm{I_{n_g}} + \mu\left(-\mathrm{I_{n_g}} + \mathrm{L_{n_g}} + \mathrm{U_{n_g}}\right)$ with I_{n_g} the identity matrix, L_{n_g} is the lower shift matrix and U_{n_g} is the upper shift matrix of dimensions $n_g \times n_g$, and $\mu = 10^{-5}$ is the mutation rate. For example, the mutation matrix Y for $n_g = 4$ has the form:

$$Y_4 = \begin{pmatrix} 1-\mu & \mu & 0 & 0 \\ \mu & 1-2\mu & \mu & 0 \\ 0 & \mu & 1-2\mu & \mu \\ 0 & 0 & \mu & 1-\mu \end{pmatrix} = \begin{pmatrix} 0.9999 & 0.0001 & 0 & 0 \\ 0.0001 & 0.9998 & 0.0001 & 0 \\ 0 & 0.0001 & 0.9998 & 0.0001 \\ 0 & 0 & 0.0001 & 0.9999 \end{pmatrix}$$

The multiplication of the patch population matrix by this symmetrical mutation matrix allows stepwise mutations to adjacent phenotypes.

Lineage is inherited uniparentally, in a mtRNA-like fashion. As a result, the frequency matrix F of all possible gamete combination can be calculated as the Kronecker product of all gamete types:

$$F = \begin{bmatrix} Q_{n_g,1} \\ Q_{n_g,2} \\ \vdots \\ Q_{n_g,n_l-1} \\ Q_{n_g,n_l} \end{bmatrix} \otimes \sum_i (Q_{g,i})^T = \begin{bmatrix} Q_{1,1} \\ \vdots \\ Q_{n_g,1} \\ Q_{1,2} \\ \vdots \\ Q_{n_g,n_l} \end{bmatrix} \otimes \begin{bmatrix} (Q_{1,1} + Q_{1,2}) & \cdots & \left(Q_{n_g,1} + Q_{n_g,2}\right) \end{bmatrix}$$

where the left term is a column matrix of frequencies of all genotype x lineage combinations (gamete type 1)and the right term is a row matrix of frequencies of all genotypes regardless of lineage (gamete type 2). The resulting frequency matrix F is replicated $n_g n_l$ times into a three-dimensional array F' of dimensions $(n_g n_l) \times n_g \times (n_g n_l)$:

$$\forall j \in \{1, \ldots, n_g n_l\}\colon F' = F_{i,g,j} = F_{i,g}$$

If i and j are the number of "1" alleles of the respective two parent genotypes, the net distribution of the number of "1" alleles k of offspring genotypes can be derived (Doebeli 1996; Barton & Shpak 2000; Shpak and Kondrashov 1999):

$$P_{k|i,j} = \sum_{L=Max[0,i+j-a]}^{Min[i,j]} \binom{i+j-2L}{k-1} \left(\frac{1}{2}\right)^{i+j-2L} \frac{\binom{i}{L}\binom{a-i}{i-L}}{\binom{a}{j}}$$

where a is the number of alleles. The resulting three-dimensional array $P_{k|i,j}$ is of dimensions $n_i \times n_j \times n_k = n_g \times n_g \times n_g$ (two parental dimensions and one offspring dimension). In order to account for different lineages, $P_{k|i,j}$ is added on the third dimensional diagonal of a null-matrix with the same dimension as F':

$$P'_{k|i,j} = \begin{cases} P_{k-(n_g\ n_l-1\ +1)\ |\ i,j-(n_g\ n_l-1\ +1)}, & (n_g\ n_l-1\ +1) \le k \le n_g \times n_l \\ & and\ (n_g\ n_l-1\ +1) \le j \le n_g \times n_l \\ 0, & else \end{cases}$$

The summation of the entrywise multiplication of both arrays, $F' P'_{k|i,j}$, along the third dimension, yields frequencies of all offspring genotype and lineage combinations. Inverse vectorization of this vector restores a matrix of original dimensions $n_g \times n_l$. The resulting frequency matrix is converted into absolute offspring contribution by multiplication with the sum of the gamete pool matrix $Q_{g,l}$:

$$\forall g \in \{1,\dots,n_g\}, l \in \{1,\dots,n_l\}, p\text{: } \mathrm{R}_{g,p,l}\ \boldsymbol{N}\ = \sum_i^{n_g} \sum_j^{n_l} \boldsymbol{Y} \times \boldsymbol{N}\ _{i,j}\ \sum_i^{n_g} \sum_j^{n_l n_g} (F'_{g,i,j} P_{g|i,j})$$

Explicit diploid multilocus model

For any diploid parent locus, the probability of producing a particular gamete is:

$$\begin{array}{cc} & \text{gamete} \\ & \begin{array}{cc} \mathbf{0} & \mathbf{1} \end{array} \\ \text{parent} \begin{array}{c} \mathbf{00} \\ \mathbf{01} \\ \mathbf{11} \end{array} & \begin{pmatrix} 1 & 0 \\ 0.5 & 0.5 \\ 0 & 1 \end{pmatrix} \end{array} \quad = \quad S_1$$

The S matrix can be generalized to a loci through the iterative entrywise multiplication of two Kronecker products:

$$\forall i \in \{1,\dots,a-1\}\text{: } S_{i+1} = \ J_{3\times 2} \otimes S_1\ \circ\ S_1 \otimes J_{3^i \times 2^i}$$

By expanding on this methodology and by incorporation of a mutation matrix Q, we can derives the fraction of offspring when multiplied by the population array $\mathbf{N}$.

3.2.2 Fitness-dependent mortality

We define the deviation from optimal adaptation A_g of genotypes with phenotypic trait values $\{z_1, \ldots, z_n\}$ in a patch with niche values $\{e_1, \ldots, e_n\}$ as the average deviation from optimal trait values:

$$A = \frac{\sum_{i=1}^{n} |e_i - z_i|}{n}$$

where n is the number of niche axes and phenotypic traits. Total mortality is a linear function of the deviation from optimal niche value A:

$$m_g = m_{min}\ 1 - A\ + m_{max} A$$

where $m_{min} = 0.001$ is the baseline mortality of optimally adapted individuals and m_{max} is the mortality of completely maladapted phenotypes. Unless otherwise stated, $m_{max} = 0.01 = 10\ m_{min}$, Maximal mortality m_{max} is equivalent to selection strength.

3.2.3 Migration

Each time step, a fraction d, the dispersal rate, of the population in each patch is displaced to neighbouring patches. A normal probability distribution function with $\sigma = 2$ is used as

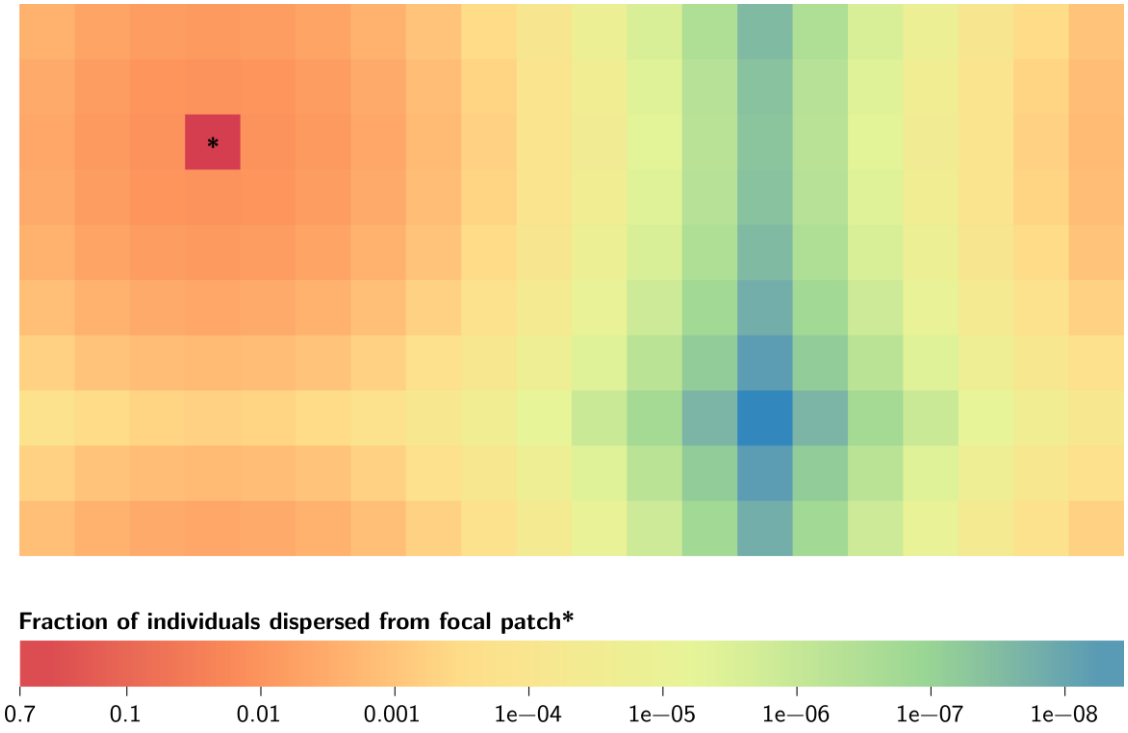

Figure 13. Hypothetical dispersal kernel for a dispersal rate of 0.3 in a landscape of 20x10 patches. 70% of the population is retained in the focal patch (indicated by *), while 30% of the individuals are redistributed over all patches based on a Gaussian dispersal kernel. Factions sum to 1. Patches are coloured based on the fraction of immigrant individuals originating from a focal patch. Due to the torus boundary conditions, the dispersal kernel is continuous at the landscape edges and connects with the opposite edge.

dispersal kernel. By only applying the dispersal kernel on the migrating fraction d of the population, varying dispersal rates only affect the magnitude of the dispersal kernel, leaving its shape invariant.

The dispersal kernel function $\mathrm{K}\ i,j\ $ calculates the fraction of all migrants of patch i that disperse to patch j, based on the distance between both patches $D_{i,j}$:

$$\forall\ i,j\ \in \{1,\ldots,n_p\}, i \neq j\text{:} \qquad \mathrm{K}\ \boldsymbol{i,j}\ = \frac{\frac{1}{\sqrt{2\pi\sigma^2}} e^{-\frac{{D_{i,j}}^2}{2\sigma^2}}}{\sum_{h=1}^{n_p} \left(\frac{1}{\sqrt{2\pi\sigma^2}} e^{-\frac{{D_{h,j}}^2}{2\sigma^2}} \right)}$$

Using the distance matrix D, containing all pairwise Euclidean or torus centroid-to-centroid distances, we can calculate a migration matrix V:

$$V_{n_p \times n_p} = \left(\ 1 - d\ \circ I_{n_p}\right) + \left(d \circ \left(1 - I_{n_p}\right) \circ \mathrm{K}\ D\ \right)$$

where I_{n_p} is the unit matrix of dimensions $n_p \times n_p$. The change in population sizes due to migration can be calculated as the difference between $N_{g,l,p}$ and the matrix multiplication of $N_{g,l,p}$ the migration matrix $V_{n_p \times n_p}$:

$$\mathrm{M}(N_{g,p,l}) = N_{g,p,l} - N_{g,p,l} \times V_{n_p \times n_p}$$

3.2.4 Stochastic extension for finite populations

The model presented above assumes infinite populations and is fully deterministic. We built an alternative stochastic model in order to relax this assumption. In the stochastic model, the maximal population size at a density of 1 in each patch is $H = 1000$ individuals. The explicit number of offspring due to reproduction during a time step are drawn from the discrete Poisson distribution with the expected value λ, given by the reproduction function $\mathrm{R}(x)$ multiplied by the integration time step Δt and conversation factor to population size H; this value is subsequently rescaled to a time step of Δt and population density by dividing through $\Delta t\, H$:

$$R^*(N_{g,p,l}) \sim \frac{Pois(\lambda = \Delta t\ H\ \mathrm{R}(N_{g,p,l}))}{\Delta t\ H}$$

The stochastic equivalent of the migration function, $\mathrm{M}^*(x)$, is given by:

$$M^*(N_{g,p,l}) \sim \frac{Pois(\lambda = \Delta t\ H\ M(N_{g,p,l}))}{\Delta t\ H}$$

3.3 Model output

Three main population descriptors are calculated and recorded for each patch: genetic load, population size and the amount of (incoming) gene flow.

Genetic load is the additive inverse of the degree of adaptation and hence, fitness. In our model, genetic load is the sum of the mutation load L_μ and migration load L_m. At equilibrium, mutation load equals the migration rate $L_\mu = \mu = 10^{-5}$ and can be considered as small relative to the migration load L_m. Therefore, in the following sections, genetic load can be considered as approximatively equivalent to migration load.

A gene flow matrix can be calculated at any given moment by a *lineage marking* procedure:

1. An empty lineage, which will act as marker lineage, is added to the population array;
2. The current population array is stored;
3. The entire population of the first patch is transferred to the marker lineage;
4. The model runs for 50 timesteps, in order to allow dispersal and gene flow of the marked population;
5. After n timesteps, the amount of individuals in the marker lineage of each patch is recorded – these are the genotypes that originated from the focal patch;
6. The obtained population array is discarded and the original population array is restored (cf. step 2);
7. Step 3 – 6 are repeated for all patches.

When this procedure is finished, the gene flow between all pairwise combinations of patches is obtained and a gene flow matrix can be constructed. For each patch, the incoming gene flow can be calculated by summing the columns of the gene flow matrix and subsequently dividing these values by the population size of the recipient patch and the number of timesteps.

3.4 General model exploration strategy

Our centre of interest lies in the dynamical changes in genetic load, population size and gene flow in the face of changes in connectivity, or more generally dispersal rates. To this end, we simulate a metapopulation inhabiting a landscape that undergoes changes in dispersal rates. Simulations start with a low population density, in which all genotypes are equally abundant in each patch. Populations are allowed to fully adapt to patch conditions during 20 000 timesteps (~200 generations for $r = 0.01$) at a dispersal rate of 0. Dispersal

rates are increased stepwise (50 steps in total) by small increments with an interval of 10 000 timesteps (~100 generations for $r = 0.01$) as stabilizing time. When a steady state equilibrium is reached, dispersal rates are decreased in an identical fashion to a dispersal rate of 0. This strategy is applied to several landscape scenarios.

In the explicit diploid model, the number of different genotypes for a loci amounts to 3^a. As a result, computational complexity increases exponentially along with the number of loci. Therefore, we use $a = 3$ loci in our simulations, resulting in a 'feasible' amount of 27 different genotypes. In the two-dimensional niche simulation, $a = 2$ loci are used, i.e. one locus per phenotypic trait.

Interrun variation in landscape-wide patterns is very low for landscapes generated under the same set of rules. Therefore, only one replicate run is shown for each scenario.

3.5 Numerical solving

Analytical tractability was lost due to the spatial extension of the model. We used the `ode.3D` function of the `R`-package `deSolve` (Soetaert *et al.* 2010) as numerical solver. Differential equations of the deterministic model were solved using a fouth-order Runge-Kutta integration method, while the stochastic model required the use of Euler integration with a fixed timestep Δt.

4 Results and discussion

4.1 Three-deme metapopulations

Before addressing more complex scenarios, we explore model dynamics by means of a simple landscape model: a three-deme metapopulation (Figure 14). This scenario consists of a metapopulation inhabiting three patches: two patches of niche type 0 and one patch of niche type 1. This causes an asymmetrical pattern of gene flow since the patch of niche type 1 is expected to experience more maladaptive gene flow relative to patches of niche type 0. As a result, this scenario closely resembles the modelled system by Kilsdonk *et al.* (*in prep.*), where one focal deme experiences disruptive gene-flow from a nonexplicit external source.

Figure 14. Three-deme landscape, featuring one patch of niche type 0 (greenblue) and two patches of niche type 1 (yellow). Numbers represent the patch ID.

For the diploid and deterministic model, increasing dispersal initially only leads to slight increases in genetic load in all patches, resulting in a limited decline in population size (Figure 15). After a critical threshold in dispersal rate, the population inhabiting the underrepresented niche type undergoes a sudden shift to a completely maladapted state. The increase in genetic load in the underrepresented niche type corresponds to a decrease in genetic load to zero in the other niche type. At this stage, standing genetic variation is completely lost in all patches. A reduction in dispersal initially does not reduce genetic load, due to the lack of standing genetic variation. Once a critical point in dispersal rate is reached, the maladapted population shifts to the well-adapted state. This point corresponds to the moment *de novo* mutations arise and can establish under the migration-selection balance.

Compared to genetic load, population size and gene flow behave very similarly and also exhibit clear hysteresis and two distinct states. For dispersal rates between both bifurcation points, two clearly distinct levels of gene flow are possible, depending on the degree of adaptation of the population. The hysteresis in gene flow thus highlights the competitive advantage of well-adapted residents, allowing reductions in gene flow, until a critical threshold in dispersal rate is reached. Due to the strong relationship between the three population descriptors, population size and gene flow patterns will only be shown if they provide additional insights to the genetic load patterns.

The obtained alternative stable states are robust to variations in parameter choice. For

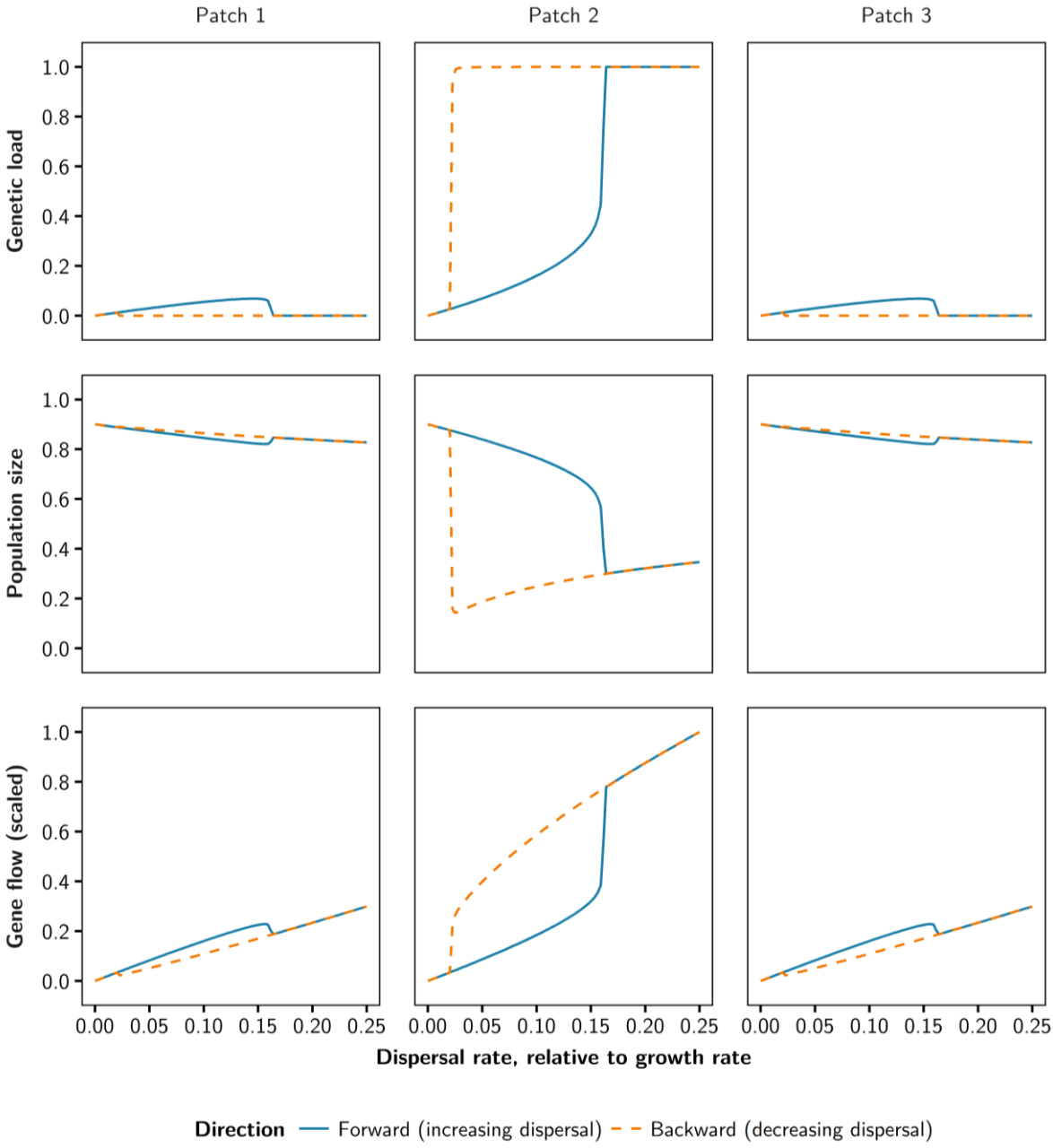

Figure 15. Genetic load, population size and gene flow in a three-deme metapopulation under increasing and decreasing dispersal, using the deterministic diploid model. Gene flow is relative to the population size of the receiving patch and scaled to 1. Dispersal rate values are expressed as fraction of the growth rate ($r = 0.01$).

the entire range of possible selection strengths (i.e. fitness-dependent mortality), hysteresis is maintained and even increases for stronger selection (Figure 16.a). For strong selection, a higher dispersal rate is required in order to reach the bifurcation point at which the population reverts to complete maladaptation, resulting in stronger hysteresis. Furthermore, hysteresis is permanent, irrespective of the time the system is allowed to stabilize (Figure 16.b).

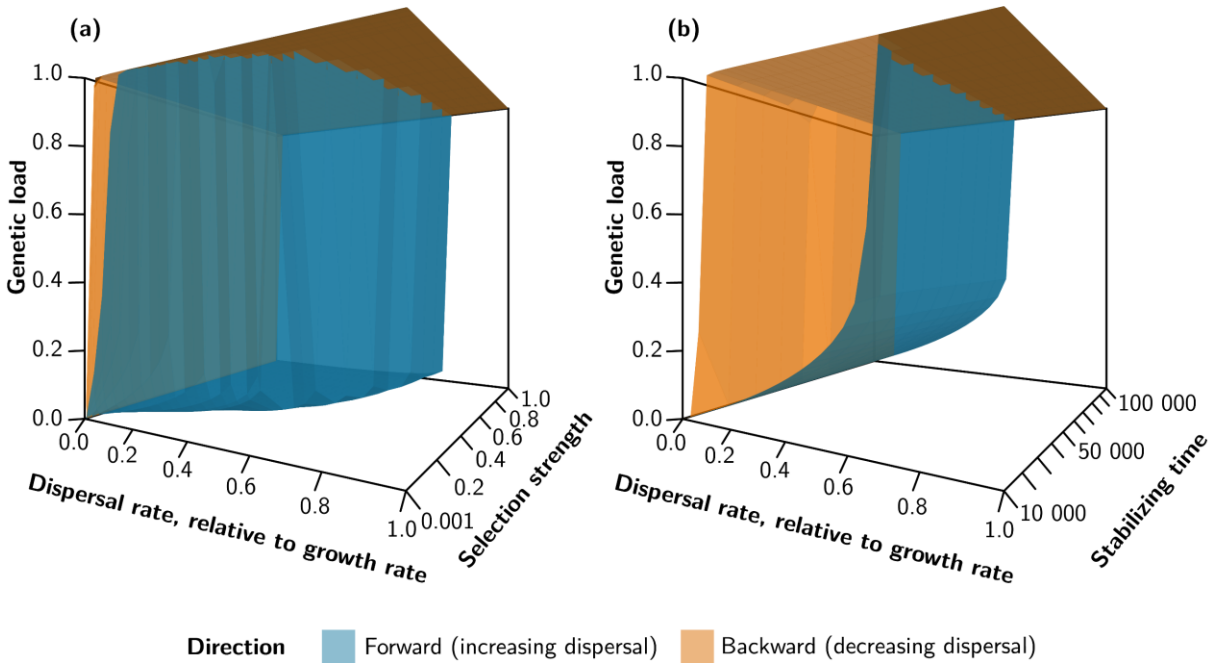

Figure 16. Maintained hysteresis in genetic load for various levels of (**a**) selection strength and (**b**) stabilizing time in a three-deme landscape. Only the results of the underrepresented niche type (niche type 1) are presented and the deterministic diploid model was used. For each value of selection strength and stabilizing time, more than one level of genetic load exists (and the blue "curtain" does not show overlap with the "orange" curtain), depending on the direction of change in dispersal rate. Dispersal rate values are expressed as fraction of the growth rate ($r = 0.01$).

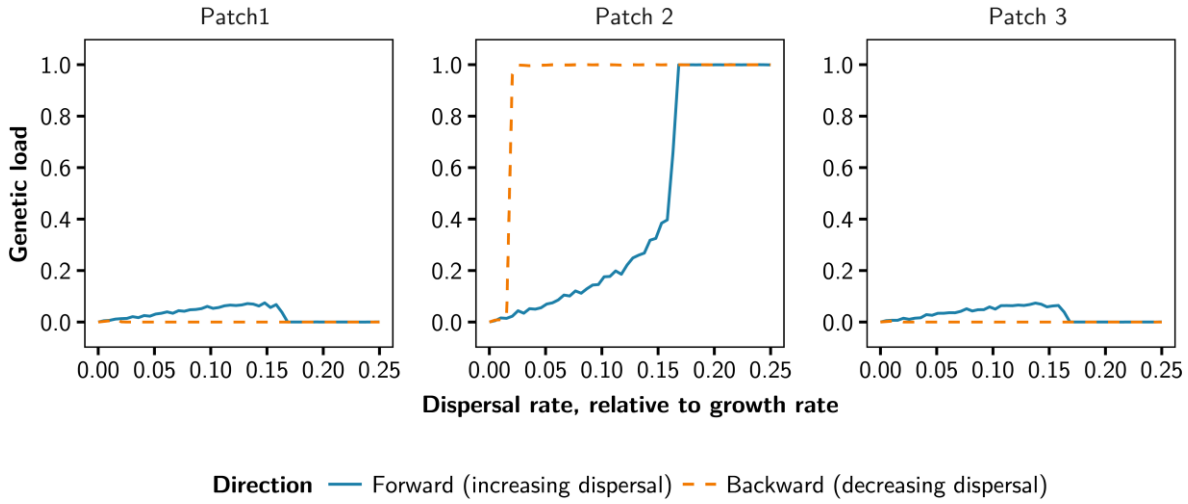

Figure 17. Genetic load in a three-deme metapopulation under increasing and decreasing dispersal, using the stochastic diploid model. Dispersal rate values are expressed as fraction of the growth rate ($r = 0.01$).

The stochastic model yields very similar results to the deterministic model (Figure 17). In subsequent scenarios, the results of the stochastic model will only be shown if considerably different from the results of the deterministic model.

The haploid (deterministic) model yields very dissimilar results compared to the diploid models (Figure 18). Genetic load gradually increases along with increasing dispersal rates

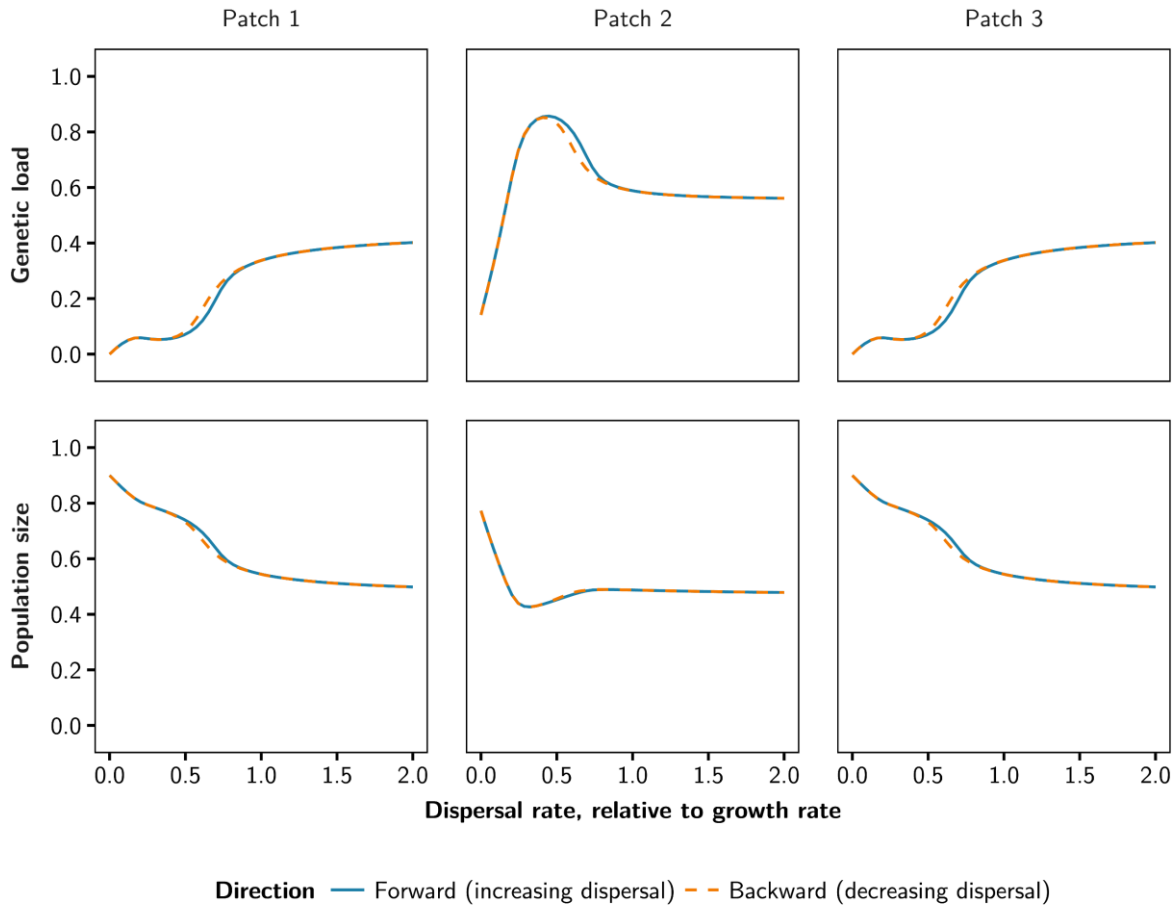

Figure 18. Genetic load in a three-deme metapopulation under increasing and decreasing dispersal, using the deterministic haploid model. Note the different x-axis scale compared to prior figures.

in the patch of the underrepresented niche type. However, no state of complete maladaptation is reached. After reaching a peak, genetic load decreases and stabilizes for high levels of dispersal. Accordingly, increases in genetic load in the two other patches are initially limited, but subsequently a rise and stabilization occurs. Some hysteresis is present when dispersal rates are reduced. The corresponding changes in population size provide a first hint at the underlying mechanism of this somewhat surprising pattern in genetic load. At high dispersal levels, homogenization of genotypes across patches is inevitable. Complete adaptation to the most abundant patch type, would cause the underrepresented niche type patch to act as a sink. The metapopulation-wide convergence towards an intermediate phenotypic value prevents linear decreases in population sizes in all patches for large dispersal rates. This pattern only appears in the haploid model and is due to the assumption of nonexplicit loci. Genotypes are defined as the number of "1" alleles across all loci and hence, a single "1" allele provides standing genetic variation for all loci. In the diploid model, the allele type at each locus is explicitly tracked and a landscape-wide loss of allelic variation for a given locus can only be reversed by a *de novo* mutation. Hereafter, we will exclusively use the diploid model.

4.2 Randomly distributed discrete niche type landscapes

In order to test whether adaptational regime shifts can persist in heterogeneous landscapes, we extend the simple three-deme metapopulation to a 200-deme landscape with two randomly distributed niche types (Figure 19).

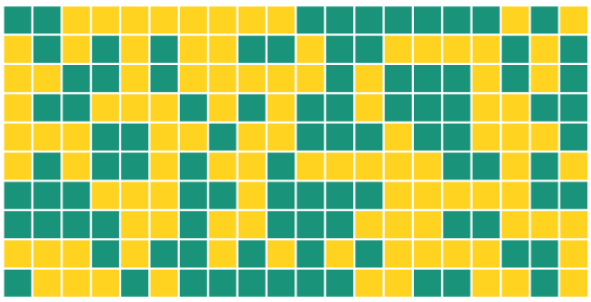

Figure 19. Landscape featuring randomly distributed patches of niche type 0 (greenblue) and patches of niche type 1 (yellow).

Adaptational regime shifts persist in this heterogeneous landscape scenario (Figure 20). The ability to resist gene flow approximatively doubled, resulting in stronger hysteresis. When a critical threshold in dispersal rate is reached, a landscape-wide shift occurs and only one phenotype persists. This phenotype corresponds to the most abundant niche type, i.e. niche type 1 in this landscape (104 patches compared to 96 patches of niche type 0). Identical patterns are obtained for replicate runs with different ratios of patches. Overall, this landscape scenario closely resembles the three-deme metapopulation, featuring the same underlying mechanisms.

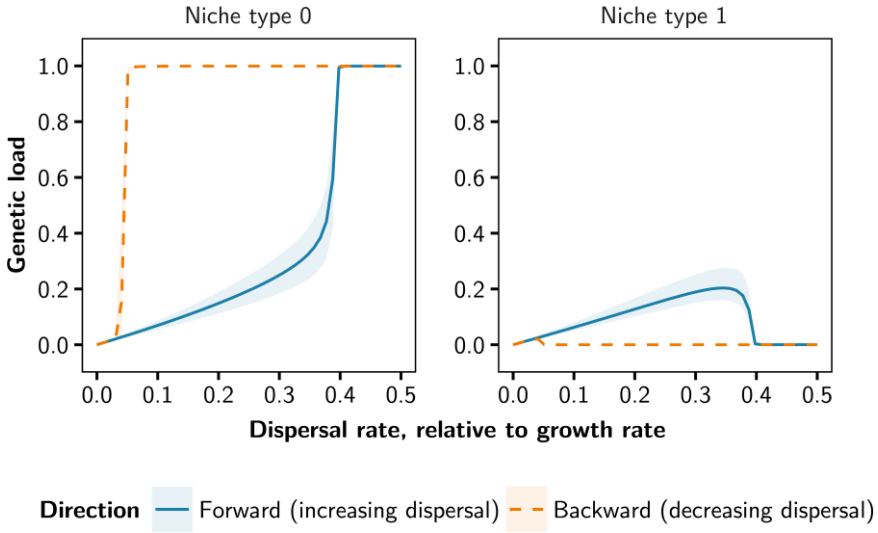

Figure 20. Average genetic load in patches of a random landscape with two niche types (0 and 1) under increasing and decreasing dispersal, using the deterministic diploid model. The shaded areas indicate 95% quantiles and represent interpatch variation in genetic load response. Dispersal rate values are expressed as fraction of the growth rate ($r = 0.01$).

4.3 Randomly distributed (semi-)continuous niche type landscapes

In this scenario, we increase the number of niche types. In a landscape with three niche types (Figure 21), hysteresis is lost and increasing dispersal rates lead to gradual increases in genetic load instead of abrupt shifts (Figure 22.a).

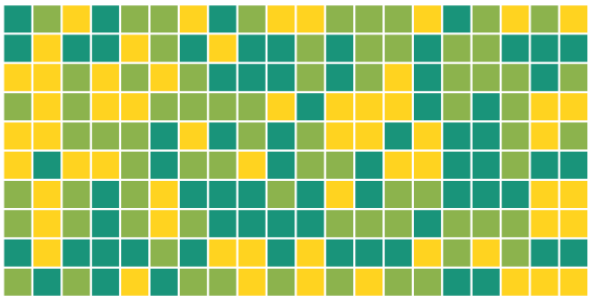

Figure 21. Landscape featuring randomly distributed patches of niche type 0 (greenblue), niche type 0.5 (green) and 1 (yellow).

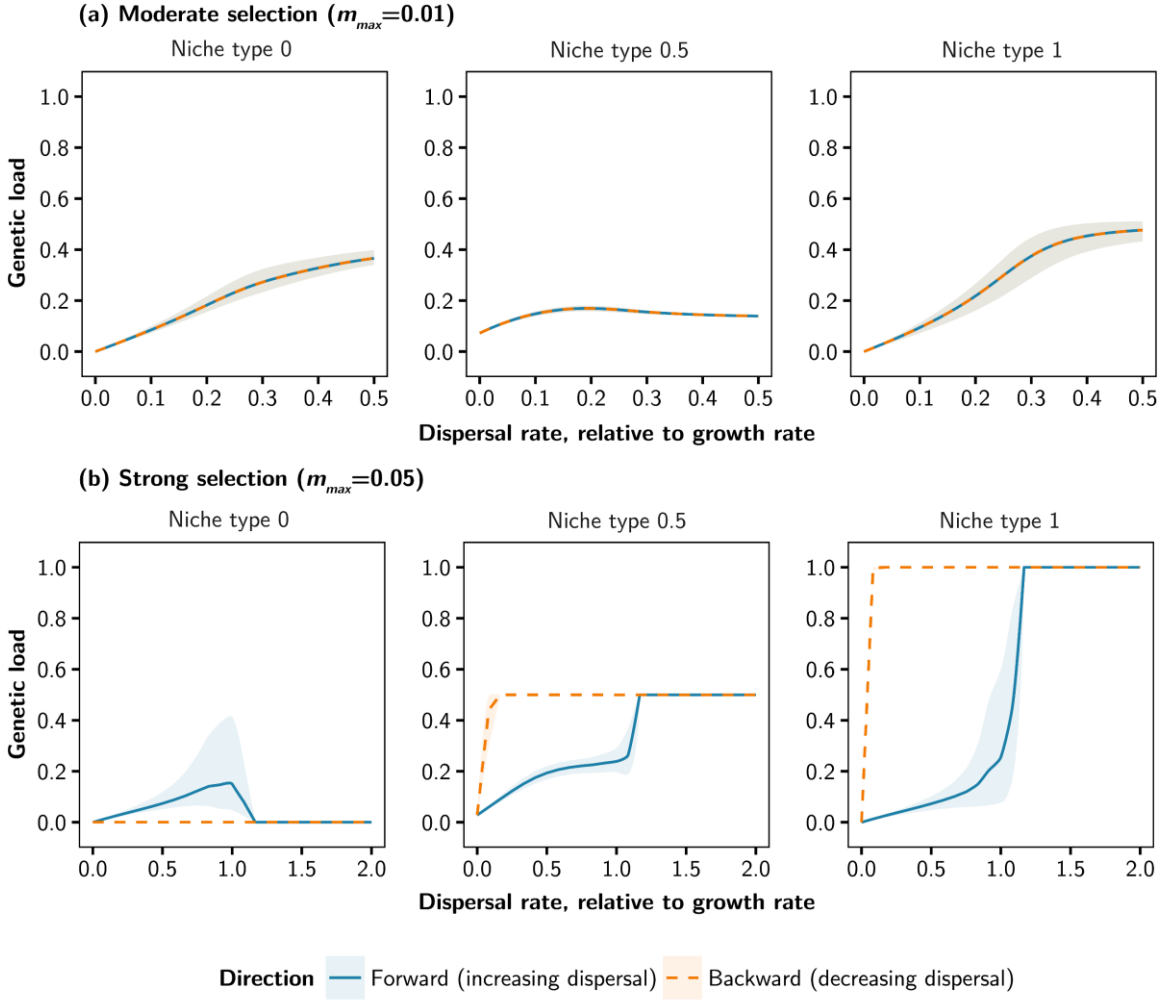

Figure 22. Genetic load in a landscape with three randomly distributed niche types under increasing and decreasing dispersal, using the deterministic diploid model. The average genetic load is shown for all patches grouped by niche type. The shaded areas indicate 95% quantiles and represent interpatch variation in genetic load response. Dispersal rate values are expressed as fraction of the growth rate ($r = 0.01$). Note the different x-axis scale for (a) and (b).

This pattern is maintained for more than three niche types (results not shown) and a continuous niche range with all possible intermediate niche types (Figure 23; Figure 24).

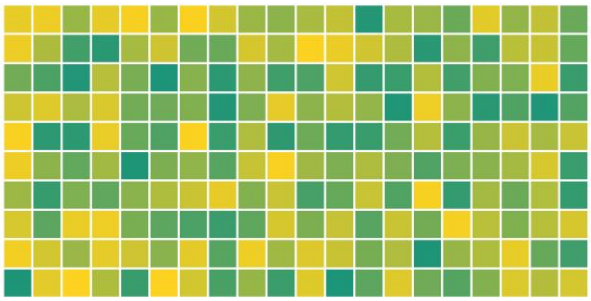

Figure 23. Landscape featuring randomly distributed niche types ranging continuously from 0 (greenblue) to 1 (yellow).

The absence of hysteresis can be explained by the reduction of environmental heterogeneity in landscapes with (semi-)continuous niche types. In these landscapes, the lower average environmental distance populations reduces the average level of selection exerted on immigrants.

Examples of both discrete and continuous niche types can be found in nature. The presence or absence of predation, invasive species, contaminants or pond turbidity, as well as many other variables can be considered as discrete binary, albeit variation might apply when present. Therefore, it is important to consider selection strength in addition to the different niche types when evaluating the possibility of adaptational regime shifts. For example, a fivefold increase in selection brings back hysteresis in the landscape scenario with three niche types (Figure 22.b). The patches of the underrepresented niche type undergo a shift to complete maladaptation when a threshold value is reached. The genetic load of intermediate patch types increases sharply when dispersal rates are increased, remains stable afterwards and increases abruptly to 0.5 when the landscape-wide shift takes place.

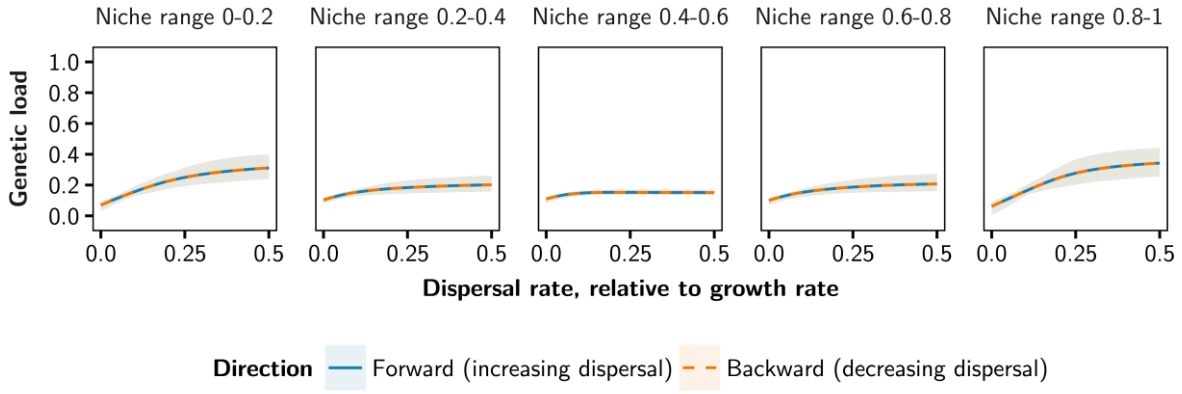

Figure 24. Genetic load in a landscape with randomly distributed continuous niche types ranging from 0 to 1, under increasing and decreasing dispersal, using the deterministic diploid model. The average genetic load is shown for patches, grouped into five niche ranges according to niche type. The shaded areas indicate 95% quantiles and represent interpatch variation in genetic load response. Dispersal rate values are expressed as fraction of the growth rate ($r = 0.01$).

In summary, the tendency towards regime shifts is diminished in landscapes with intermediary transitions between niche types. In these landscapes, genetic load tends to increase gradually, from system-wide adaptation to system-wide maladaptation. Our results are in close agreement with the general predictions regarding the stability of networks depending on their topology and interactions, as outlined by Scheffer *et al.* (2012). In general, compartmentalized and heterogeneous networks tend to be behave gradually in response to change, in contrast to networks with low modularity and more gradual connections, which are more robust to change. However, if interactions are antagonistic (e.g. competition), compartmentalized and heterogeneous networks tend to be more robust. In our model system, the relationship between demes in heterogeneous landscapes is antagonistic. Our findings suggest that landscapes with discrete niche types, corresponding to high modularity, are indeed more robust to change, i.e. genetic load increases slightly when dispersal rates increase. This is in close agreement with the general predictions of Scheffer *et al.* (2012).

4.4 Multidimensional niche type landscapes

In this scenario, we determine whether the presence of multiple niche axes enhances the potential of residents to resist to gene flow dispersal rates. More specifically, we compare two landscapes in which four niches are distributed along one niche axis (landscape not shown, equivalent to Figure 21 with four niche types instead of three) or two niche axes (Figure 24).

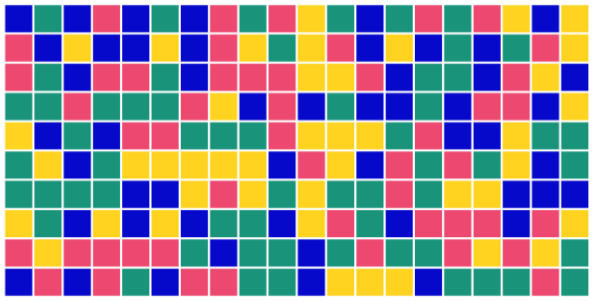

Figure 24. Landscape featuring randomly distributed patches of two-dimensional niche types with two niche types along each niche axis, resulting in four distinct niche types. Yellow patches represent niche types 1 & 1, green patches niche types 0 & 1, pink patches niche types 1 & 0 and blue patches niche types 0 & 0.

In line with previous results, we do not find hysteresis in genetic load patterns when the four niche types are structured along one niche axis (Figure 25). In contrast, hysteresis and adaptational regime shifts emerge when the four niche types are distributed along two distinct niche axis. Along each niche axis, the patches of the underrepresented niche type undergo an abrupt shift to complete maladaptation.

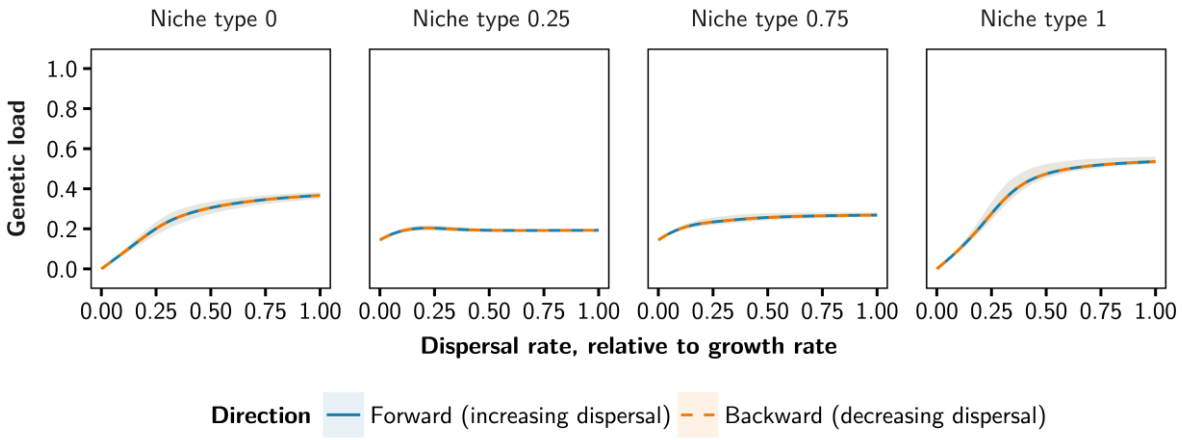

Figure 25. Landscape featuring randomly distributed patches of niche type 0 (greenblue), niche type 0.5 (green) and 1 (yellow).

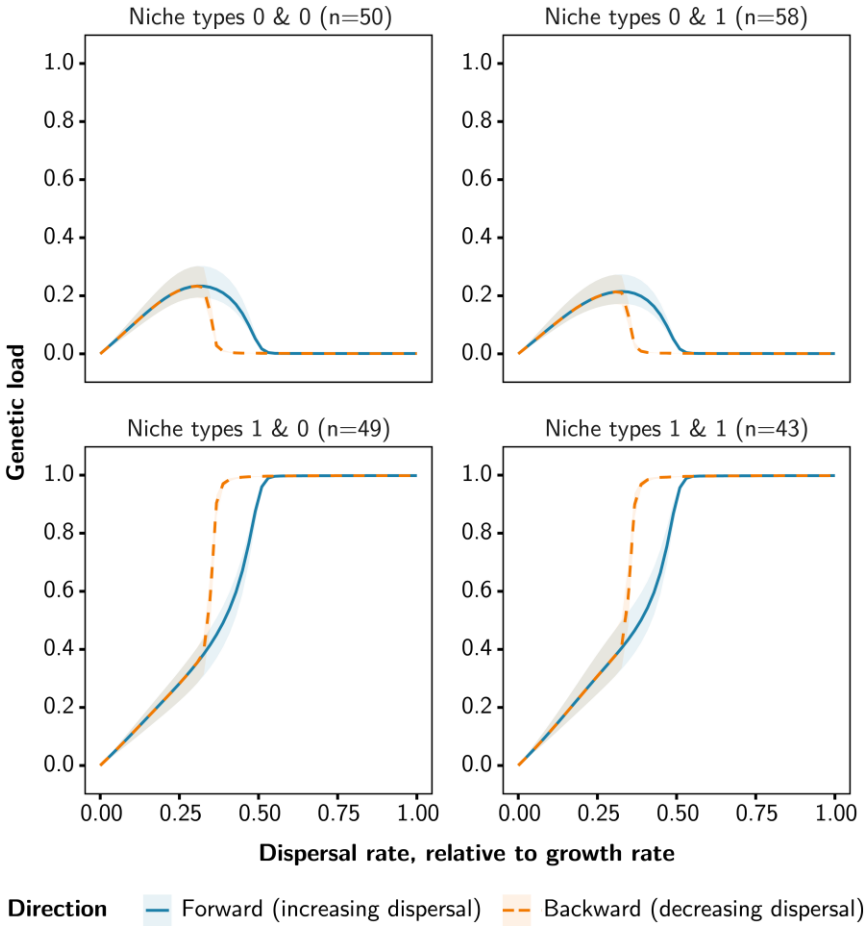

Figuur 26. Genetic load in a landscape with two niche axis and two niche types per niche axis, under increasing and decreasing dispersal, using the deterministic diploid model. The average genetic load is shown for all patches grouped by niche type. The number of patches of each niche type is printed between brackets. The shaded areas indicate 95% quantiles and represent interpatch variation in genetic load response. Dispersal rate values are expressed as fraction of the growth rate ($r = 0.01$).

4.5 Aggregated niche type landscapes and synchronicity with refugia

Usually, the distribution of niche types across space is non-random. By means of a landscape with spatially aggregated niche types (Figure 27), we determine the effect of niche type clusters on the patterns of adaptation when dispersal rates are changed. In addition, we examine adaptive patterns in patches that are spatially separated from the core clusters of the corresponding niche type. These patches are equivalent to refugia.

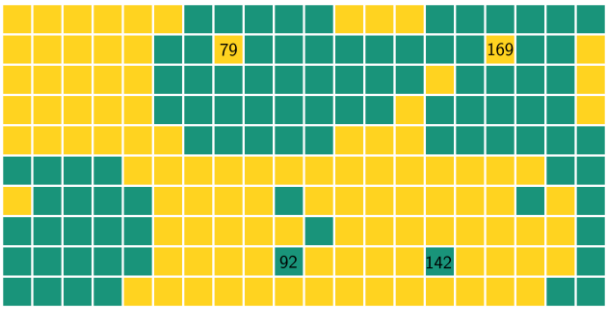

Figure 27. Landscape featuring two spatially aggregated niches. In addition, some refugia patches are present with opposite niche types compared to their neighbouring patches. Refugia patches are numbered to allow individual identification.

Spatial aggregations of niche types increases the resistance of patches to gene flow (Figure 28). Interestingly, refugia patches show high synchronicity with the core area of their corresponding niche type, despite being surrounded by patches of opposite niche types, highlighting the systemic and landscape wide impact of adaptational regime shifts. Obviously, when genetic variation is lost at a landscape-wide scale, corresponding patterns in gene flow are trivial. However, synchronicity is also evident before standing genetic variation is lost.

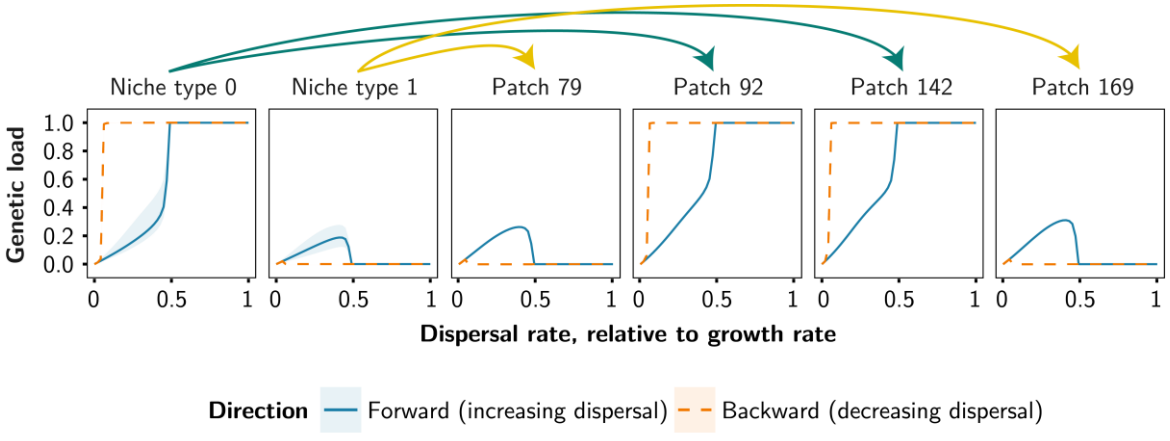

Figuur 28. Genetic load in a landscape with two spatially aggregated niche types, under increasing and decreasing dispersal, using the deterministic diploid model. The average genetic load is shown for all patches of both niche types (two panels at the left). The shaded areas indicate 95% quantiles and represent interpatch variation in genetic load response. The four right panels show individual patterns in genetic load for selected refugia patches. Arrows represent the niche type the refugia patches belong to. Dispersal rate values are expressed as fraction of the growth rate ($r = 0.01$).

4.6 Niche alterations in heterogeneous landscapes

Finally, we also evaluate the effect of perturbations. In a landscape with spatially aggregated niche types (identical to Figure 27 without refugia patches), patches of niche type 1 are gradually altered to niche type 0, based on a Bernoulli trial for each patch at each timestep with a probability of $p_{alter} = 0.00005$. The simulation takes place at a dispersal rate of $d = 0.001$, which initially allows near-optimal adaptation in each patch. Initially, genetic load in patches increases only slightly. After a critical threshold in patch alteration is reached, a landscape-wide shift takes place and populations inhabiting the niche type that is being altered, undergo complete maladaptation. This finding is highly relevant in the current context of human-induced changes and habitat alteration, since it indicates that these changes can possibly result in catastrophic effects at the level of subpopulations.

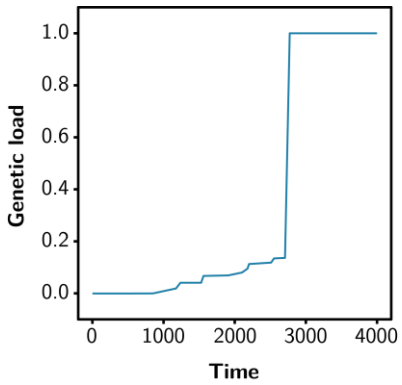

Figure 29. Changes in average genetic load through time in patches of the niche type that is being altered, using the diploid deterministic model.

4.7 Global findings

By coupling an evolutionary metapopulation model with randomly generated landscapes, we were able to elucidate several key elements that determine and influence the occurrence of adaptational regime shifts in spatially structured landscapes. We found that the regime shifts observed in simple systems, for example a three-deme system, persist in heterogeneous landscapes and are even reinforced. In addition, our results also show that locally adapted populations succeed in reducing maladaptive gene flow in the face of increasing dispersal rates. A common pattern throughout most scenarios is the complete maladaptation that takes place in the underrepresented niche type, while populations inhabiting the most abundant niche type gain and maintain complete local adaptation.

In agreement with prior work on regime shifts in spatial systems, we found that the availability of intermediate niche types reduces robustness to gene flow and yields very gradual transitions to systemic maladaptation. In contrast, we find that regime shifts are more likely to occur in landscapes with niches that are distributed along multiple niche

axes, compared to when variation in niche types is situated along a unidimensional niche axis. Spatial aggregation of niche types reinforces the occurrence regime shifts. Interestingly, refugia patches surrounded by patches with an alternative niche types, show full synchronicity with patches of corresponding niche types that form a core area.

Finally, we identify abrupt shifts in the degree of adaptation following alterations in niche types.

4.8 Further directions

We only performed analyses on landscapes without empty patches. Empty patches, where no individuals can establish or grow, would allow to incorporate the effects of isolation and gradients in isolation. Unfortunately, the model definition of migration does not allow for empty patches in simulations where dispersal rates are changed. Empty patches would induce artefacts through dispersal-rate dependent mortality, since individuals cannot establish and die when dispersed to empty patches. Active rather than passive dispersal would partially circumvent this issue. Active dispersal would however also fail to properly address the effect of patch isolation. Another alternative is to consider species with high reproductive rates, which would reduce the negative impact of dispersal towards empty patches on population sizes. The artefact-free inclusion of empty niches would largely increase the ability of the model to generate insights into the occurrence of eco-evolutionary regime shifts in natural landscapes that face threats like habitat destruction.

An additional extension to the model would consist of landscape-wide changes in niche type in order to simulate processes like climate change and their impact on adaptive dynamics of populations in heterogeneous landscapes.

5 References

Bel G, Hagberg A, Meron E (2012) Gradual regime shifts in spatially extended ecosystems. *Theoretical Ecology*, **5**, 591–604.

Boileau MG, Hebert PDN, Schwartz SS (1992) Non-equilibrium gene frequency divergence : founder effects in natural populations persistent. *J. evol. Biol.*, **39**, 25–39.

Boughton DA (1999) Empirical evidence for complex source-sink dynamics with alternative states in a butterfly metapopulation. *Ecology*, **80**, 2727–2739.

Bourne EC, Bocedi G, Travis JMJ *et al.* (2014) Between migration load and evolutionary rescue: dispersal, adaptation and the response of spatially structured populations to environmental change. *Proceedings of the Royal Society B: Biological Sciences*, **281**, 20132795–20132795.

Bridle JR, Vines TH (2007) Limits to evolution at range margins: when and why does adaptation fail? *Trends in Ecology and Evolution*, **22**, 140–147.

Brown JH, Mehlman DW, Stevens GC (1995) Spatial Variation in Abundance. *Ecology*, **76**, 2028–2043.

Butchart S, Walpole M, Collen B *et al.* (2010) Global Biodiversity : Indicators of Recent Declines. *Science*, **328**, 1164–1168.

Carpenter SR, Ludwig D, Brock WA (1999) Management of Eutrophication for Lakes Subject tot Potentially Irreversible Change. *Ecological Applications*, **9**, 751–771.

Crespi BJ (2004) Vicious circles: Positive feedback in major evolutionary and ecological transitions. *Trends in Ecology and Evolution*, **19**, 627–633.

Dobzhansky T (1937) *Genetics and the origin of species*. Columbia University Press, New York.

Donahue MJ, Desharnais R a., Robles CD, Arriola P (2011) Mussel Bed Boundaries as Dynamic Equilibria: Thresholds, Phase Shifts, and Alternative States. *Ther American Naturalist*, **178**, 612–625.

Van Donk E, Van de Bund WJ (2002) Impact of submerged macrophytes including charophytes on phyto- and zooplankton communities: Allelopathy versus other mechanisms. *Aquatic Botany*, **72**, 261–274.

Edelaar P, Bolnick DI (2012) Non-random gene flow: An underappreciated force in evolution and ecology. *Trends in Ecology and Evolution*, **27**, 659–665.

Endler JA (1986) Gene Flow and Population Differentiation. *Science*, **179**, 243–250.

Farkas TE, Mononen T, Comeault AA, Nosil P (2016) Observational evidence that

maladaptive gene flow reduces patch occupancy in a wild insect metapopulation. *Evolution*, **70**, 2879–2888.

Felsenstein J (1977) Multivariate normal genetic models with a finite number of loci. In: *Proceedings of the International Conference on Quantitative Genetics* (ed Pollak E), pp. 227–426. Iowa State University Press.

Flaxman SM, Wacholder AC, Feder JL, Nosil P (2014) Theoretical models of the influence of genomic architecture on the dynamics of speciation. *Molecular Ecology*, **23**, 4074–4088.

Gardner RH, Milne BT, Turnei MG, O'Neill R V. (1987) Neutral models for the analysis of broad-scale landscape pattern. *Landscape Ecology*, **1**, 19–28.

Gomulkiewicz R, Holt RD (1995) When does evolution by natural selection prevent extinction? *Evolution*, **49**, 201–207.

Gonzalez A, Ronce O, Ferriere R, Hochberg ME (2012) Evolutionary rescue : an emerging focus at the intersection between ecology and evolution. *Philosophical Transactions of the Royal Society B: Biological Sciences*, **368**.

Greenwood PJ (1980) Mating systems, philopatry and dispersal in birds and mammals. *Animal Behaviour*, **28**, 1140–1162.

Grimm MP (1989) Northern pike (*Esox lucius* L.) and aquatic vegetation, tools in the management of fisheries and water quality in shallow waters. *Hydrobiological Bulletin*, **23**, 59–65.

Hendry AP, Taylor EB (2004) How much of the variation in adaptive divergence can be explained by gene flow? An evaluation using lake-stream stickleback pairs. *Evolution*, **58**, 2319–2331.

Hilt S, Köhler J, Kozerski HP, van Nes EH, Scheffer M (2011) Abrupt regime shifts in space and time along rivers and connected lake systems. *Oikos*, **120**, 766–775.

Holling CS (1973) Resilience and stability of ecological systems. *Annual Review of Ecology and Systematics*, **4**, 1–23.

Holling CS (1996) Engineering Resilience versus Ecological Resilience. In: *Engineering within ecological constraints* (ed Schulze P), pp. 31–44. NATIONAL ACADEMY PRESS, Washington, D.C.

Holt RD, Keitt TH, Lewis M a, Maurer B a, Taper ML (2005) Theoretical models of species' borders: single species approaches. *Oikos*, **108**, 18–27.

Jenkins DG, Carey M, Czerniewska J *et al.* (2010) A meta-analysis of isolation by distance: Relic or reference standard for landscape genetics? *Ecography*, **33**, 315–320.

Jeppesen E, Jensen JP, Søndergaard M *et al.* (1997) Top-down control in freshwater lakes : the role of nutrient state , submerged macrophytes and water depth. *Hydrobiologia*, **342**, 151–164.

Kéfi S, Holmgren M, Scheffer M (2016) When can positive interactions cause alternative stable states in ecosystems? *Functional Ecology*, **30**, 88–97.

Keitt TH, Lewis MA, Holt RD (2001) Allee effects, invasion pinning, and species' borders. *The American naturalist*, **157**, 203–16.

Kennedy PG, Peay KG, Bruns TD *et al.* (2016) Root tip competition among ectomycorrhizal fungi: are priority fffects a rule or an exception? *Ecology*, **90**, 2098–2107.

Kimura M (1983) *The neutral theory of molecular evolution*. Cambridge University Press, Cambridge.

Van de Koppel J, Rietkerk M, Van Langevelde F *et al.* (2002) Spatial heterogeneity and irreversible vegetation change in semiarid grazing systems. *The American naturalist*, **159**, 209–218.

Van De Leemput IA, Nes EH Van, Scheffer M (2015) Resilience of Alternative States in Spatially Extended Ecosystems. *PloS one*, **10**, 1–17.

Lehtonen J, Kokko H (2012) Positive feedback and alternative stable states in inbreeding, cooperation, sex roles and other evolutionary processes. *Philosophical Transactions of the Royal Society B: Biological Sciences*, **367**, 211–221.

Lenormand T (2002) Gene flow and the limits to natural selection. *Trends in Ecology and Evolution*, **17**, 183–189.

Lopez S, Rousset F, Shaw FH, Shaw RG, Ronce O (2009) Joint effects of inbreeding and local adaptation on the evolution of genetic load after fragmentation. *Conservation Biology*, **23**, 1618–1627.

Lynch M, Gabriel W (1990) Mutation Load and the Survival of Small Populations. *Evolution*, **44**, 1725–1737.

Manel S, Holderegger R (2013) Ten years of landscape genetics. *Trends in Ecology and Evolution*, **28**, 614–621.

Manel S, Schwartz MK, Luikart G, Taberlet P (2003) Landscape genetics: Combining landscape ecology and population genetics. *Trends in Ecology and Evolution*, **18**, 189–197.

May RM (1977) Thresholds and breakpoints in ecosystms with a multiplicity of stable states. *Nature*, **260**, 471–477.

Mayr E (1942) *Systematics and the origin of species, the viewpoint of a zoologist.*

De Meester L, Gómez A, Okamura B, Schwenk K (2002) The Monopolization Hypothesis and the dispersal–gene flow paradox in aquatic organisms. *Acta Oecologica*, **23**, 121–135.

De Meester L, Vanoverbeke J, Kilsdonk LJ, Urban MC (2016) Evolving Perspectives on Monopolization and Priority Effects. *Trends in Ecology and Evolution*, **31**, 136–146.

Meijer ML, de Haan MW, Breukelaar AW, Buiteveld H (1990) Is reduction of the benthivorous fish an important cause of high transparency following biomanipulation in shallow lakes? *Hydrobiologia*, **200–201**, 303–315.

Meirmans PG (2012) The trouble with isolation by distance. *Molecular Ecology*, **21**, 2839–2846.

Mergeay J, De Meester L, Eggermont H, Verschuren D (2011) Priority effects and species sorting in a long paleoecological record of repeated community assembly through time. *Ecology*, **92**, 2267–2275.

Moore JS, Gow JL, Taylor EB, Hendry AP (2007) Quantifying the constraining influence of gene flow on adaptive divergence in the lake-stream threespine stickleback system. *Evolution*, **61**, 2015–2026.

Moore JS, Hendry AP (2005) Both selection and gene flow are necessary to explain adaptive divergence: Evidence from clinal variation in stream stickleback. *Evolutionary Ecology Research*, **7**, 871–886.

Van Nes EH Van, Scheffer M (2005) Implications of Spatial Heterogeneity for Catastrophic Regime Shifts in Ecosystems. *Ecology*, **86**, 1797–1807.

Nosil P (2004) Reproductive isolation caused by visual predation on migrants between divergent environments. *Proceedings of the Royal Society B: Biological Sciences*, **271**, 1521–1528.

Nosil P, Crespi BJ (2004) Does gene flow constrain adaptive divergence or vice versa? A test using ecomorphology and sexual isolation in Timena cristinae walking-sticks. *Evolution*, **58**, 102–112.

Nosil P, Feder JL, Flaxman SM, Gompert Z (2017) Tipping points in the dynamics of speciation. *Nature Ecology & Evolution*, **1**, 1.

Nosil P, Sandoval CP (2008) Ecological niche dimensionality and the evolutionary diversification of stick insects. *PLoS ONE*, **3**.

Nosil P, Vines TH, Funk DJ (2005) Perspective: Reproductive Isolation Caused By Natural Selection Against Immigrants From Divergent Habitats. *Evolution*, **59**, 705–719.

Orsini L, Mergeay J, Vanoverbeke J, De Meester L (2013a) The role of selection in driving landscape genomic structure of the waterflea Daphnia magna. *Molecular Ecology*, **22**, 583–601.

Orsini L, Vanoverbeke J, Swillen I, Mergeay J, De Meester L (2013b) Drivers of population genetic differentiation in the wild: Isolation by dispersal limitation, isolation by adaptation and isolation by colonization. *Molecular Ecology*, **22**, 5983–5999.

Postma E, van Noordwijk AJ (2005) Gene flow maintains a large genetic difference in clutch size at a small spatial scale. *Nature*, **433**, 65–68.

R Core Team (2016) R: A Language and Environment for Statistical Computing.

Ramachandran S, Deshpande O, Roseman CC *et al.* (2005) Support from the relationship of genetic and geographic distance in human populations for a serial founder effect originating in Africa. *Proceedings of the National Academy of Sciences of the United States of America*, **102**, 15942–15947.

Räsänen K, Hendry AP (2008) Disentangling interactions between adaptive divergence and gene flow when ecology drives diversification. *Ecology Letters*, **11**, 624–636.

Rice WR, Hostert EE (1993) Laboratory Experiments on Speciation: What Have We Learned in 40 Years? *Evolution*, **47**, 1637–1653.

Richardson JL, Urban MC, Bolnick DI, Skelly DK (2014) Microgeographic adaptation and the spatial scale of evolution. *Trends in Ecology and Evolution*, **29**, 165–176.

Ronce O, Kirkpatrick M (2001) When sources become sinks: migrational meltdown in heterogeneous habitats. *Evolution*, **55**, 436–438.

De Roos AM, Boukal DS, Persson L (2006) Evolutionary regime shifts in age and size at maturation of exploited fish stocks. *Proceedings. Biological sciences / The Royal Society*, **273**, 1873–80.

Rundle HD, Whitlock MC (2001) A genetic interpretation of ecologically dependent isolation. *Evolution*, **55**, 198–201.

Scheffer M (1990) Multiplicity of stable staes in freshwater systems. *Hydrobiologia*, **200**, 475–486.

Scheffer M, Bascompte J, Brock WA *et al.* (2009) Early-warning signals for critical transitions. *Nature*, **461**, 53–59.

Scheffer M, van den Berg M, Breukelaar A *et al.* (1994) Vegetated areas with clear water in turbid shallow lakes. *Aquatic Botany*, **49**, 193–196.

Scheffer M, Carpenter SR (2003) Catastrophic regime shifts in ecosystems: Linking theory to observation. *Trends in Ecology and Evolution*, **18**, 648–656.

Scheffer M, Carpenter SR, Dakos V, Nes EH van (2015) Generic indicators of ecological resilience: inferring the chance of a critical transition. *Annual Review of Ecology, Evolution, and Systematics*, **46**, 145–167.

Scheffer M, Carpenter S, Foley J a, Folke C, Walker B (2001) Catastrophic shifts in ecosystems. *Nature*, **413**, 591–6.

Scheffer M, Carpenter SR, Lenton TM *et al.* (2012) Anticipating Critical Transitions. *Science*, **338**, 344–348.

Scheffer M, Hosper SH, Meijer M-L, Moss B, Jeppesen E (1993) Alternative Equilibria in Shallow Lakes. *Trends in Ecology & Evolution*, **8**, 275–279.

Schluter D (1996) Ecological causes of adaptive radiation. *The American Naturalist*, **148**, S40–S64.

Schluter D (2000) *The Ecology of Adaptive Radiation*. Oxford University Press, Oxford.

Schreiber SJ (2015) Coexistence in Systems With Apparent Competition. *Natural Resource Modelling*, **28**, 475–496.

Schröder A, Persson L, Roos ADAM De, De Roos AM (2005) Direct experimental evidence for alternative stable states: a review. *Oikos*, **110**, 3–19.

Siteur K, Eppinga MB, Doelman A, Siero E, Rietkerk M (2016) Ecosystems off track: rate-induced critical transitions in ecological models. *Oikos*, **125**, 1689–1699.

Slatkin M (1987) Gene flow and the geographic structure of populations. *Science*, **236**, 787–792.

Smith VH, Tilman GD, Nekola JC (1998) Eutrophication: Impacts of excess nutrient inputs on freshwater, marine, and terrestrial ecosystems. *Environmental Pollution*, **100**, 179–196.

Soetaert K, Petzoldt T, Woodrow Setzer R (2010) Solving Differential Equations in R : Package deSolve. *Journal of Statistical Software February*, **33**.

Søndergaard M, Jeppesen E, Lauridsen TL *et al.* (2007) Lake restoration : successes , failures and long-term effects. *Journal of Applied Ecology*, **44**, 1095–1105.

Storfer A, Murphy MA, Evans JS *et al.* (2007) Putting the “landscape” in landscape genetics. *Heredity*, **98**, 128–142.

Storfer A, Murphy MA, Spear SF, Holderegger R, Waits LP (2010) Landscape genetics: Where are we now? *Molecular Ecology*, **19**, 3496–3514.

Tackenberg O, Poschlod P, Kahmen S (2003) Dandelion Seed Dispersal: The Horizontal Wind Speed Does Not Matter for Long-Distance Dispersal - It is Updraft! *Plant Biology*, **5**, 451–454.

Thomas CD, Kunin WE (1999) The spatial structure of populations. *J Anim Ecology*, **68**, 647–657.

Urban MC, Leibold MA, Amarasekare P *et al.* (2008) The evolutionary ecology of metacommunities. *Trends in Ecology and Evolution*, **23**, 311–317.

Urban MC, De Meester L (2009) Community monopolization: local adaptation enhances priority effects in an evolving metacommunity. *Proceedings. Biological sciences / The Royal Society*, **276**, 4129–38.

Vanoverbeke J, Urban MC, De Meester L (2016) Community assembly is a race between immigration and adaptation: eco-evolutionary interactions across spatial scales. *Ecography*, **39**, 858–870.

Ventura M, Petrusek A, Miró A *et al.* (2014) Local and regional founder effects in lake zooplankton persist after thousands of years despite high dispersal potential. *Molecular Ecology*, **23**, 1014–1027.

Williams HTP, Lenton TM (2010) Evolutionary regime shifts in simulated ecosystems. *Oikos*, **119**, 1887–1899.

Wright S (1943) Isolation by Distance. *Genetics*, **28**, 114–138.

Wright S (1946) Isolation by distance under diverse systems of mating. *Genetics*, **31**, 39–59.

Addendum 1: Risk analysis

No biological, chemical or physical risks are associated with this thesis, considering its computational nature. However, some risks related to prolonged computer work need to be considered. Hereafter, the most important health concerns along with mitigating measures according to the Belgian Safe Work Information Center[1] (BeSWIC) are presented.

Long periods of sitting in poor positions can induce back pain. A proper body posture, frequent movements and a comfortable and firm chair reduce chances of developing backpain.

Unsuitable table top height, distant keyboard and mouse and inappropriate display setup might lead to neck and shoulder pain. The workspace should be arranged optimally in order to reduce neck and shoulder load. The workspace should be tidy in order to allow free movement.

The use of a mouse touchpad can avoid complaints related to elbows, wrists and fingers complaints.

Prolonged exposure to electronic monitors can cause eye strains, dryness or twitches. Sufficiently large screen and character size, appropriate eye-to-screen distance and well-adjusted screen brightness are important in order to avoid eye problems.

Extensive periods of sitting increase sensitivity to air-currents, bad air quality and temperature fluctuations. Frequent aerations and a proper radiator adjustment should ensure an optimal working environment.

[1] www.beswic.be

ECOLOGY, EVOLUTION AND BIODIVERSITY CONSERVATION
Charles Deberiotstraat 32 – box 2439
3000 LEUVEN, BELGIË
tel. + 32 16 00 00 00
fax + 32 16 00 00 00
www.kuleuven.be